

*P
2mit*

**NASA TECHNICAL
MEMORANDUM**

NASA TM X-71931
COPY NO.

NASA TM X-71931

(NASA-TM-X-71931) PRELIMINARY STATIC
TESTS OF A SIMULATED UPPER-SURFACE BLOWN
JET-FLAP CONFIGURATION UTILIZING A
FULL-SIZE TURBOFAN ENGINE (NASA) 44 p
HC \$5.25

N74-20638

Unclass
CSCL 01A G3/01 35338

PRELIMINARY STATIC TESTS OF A SIMULATED UPPER-SURFACE BLOWN JET-FLAP
CONFIGURATION UTILIZING A FULL-SIZE TURBOFAN ENGINE

By

James P. Shivers and Charles C. Smith, Jr.

March 1974

This informal documentation medium is used to provide accelerated or special release of technical information to selected users. The contents may not meet NASA formal editing and publication standards, may be revised, or may be incorporated in another publication.

**NATIONAL AERONAUTICS AND SPACE ADMINISTRATION
LANGLEY RESEARCH CENTER, HAMPTON, VIRGINIA 23665**

PRELIMINARY STATIC TESTS OF A SIMULATED
UPPER-SURFACE BLOWN JET-FLAP CONFIGURATION
UTILIZING A FULL-SIZE TURBOFAN ENGINE

By James P. Shivers and Charles C. Smith, Jr.

SUMMARY

A preliminary investigation has been conducted to evaluate the static turning performance and the pressure and temperature environment of an upper-surface blown (USB) wing and flap utilizing a small (2,200-lb thrust) turbofan engine. The static test configuration employed the propulsion system and the wing and flap design of a large USB wind-tunnel model. The exhaust nozzle was a fixed design intended to provide attached flow on the upper surface of the wing-flap system. This nozzle was rectangular in shape and had an aspect ratio (width/height) of 6.0. Results were obtained for several modifications of the hot core (primary) nozzle and for a range of flap deflections and thrust conditions. An acceptable compromise between static turning performance and surface temperature constraints was obtained with an elliptical primary nozzle which replaced the originally designed round primary nozzle. Measurements of flow characteristics over the wing and flap surfaces indicated attached flow even with the largest flap deflections and revealed a very rapid decay of peak velocities from the exhaust nozzle to the flap trailing edge.

INTRODUCTION

As part of a general research program to provide fundamental information on the upper-surface blown (USB) jet-flap concept, the present investigation was conducted to evaluate static turning performance as well as the pressure and temperature environment on a USB wing and flap utilizing a small (2,200-lb thrust) turbofan engine. The apparatus used in this investigation was an outdoor static test stand supporting a JT-15D-1 turbofan engine which was

equipped with a canted rectangular nozzle of aspect-ratio-6.0 and which was oriented to cause the thrust to be directed onto the upper surface of a boiler-plate wing-flap system. The test configuration was an adaptation of the propulsion system and wing/flap design of a large twin-engine USB wind-tunnel model which is to be tested in the Langley full-scale tunnel. The primary objective of the investigation was to establish a configuration that would provide acceptable static turning performance over the desired range of flap deflection angles. Inasmuch as the wind-tunnel model is to utilize the wing structure of an existing general aviation aircraft, the temperature environment on the upper surface of the wing and flap was a prime consideration. The investigation involved modifications of the initial primary, or core, nozzle designed to alleviate high temperature problems on the wing and flap upper surfaces. The investigation also included surface pressure measurements on the wing and flaps aft of the rectangular nozzle which provide indications of attached flow and which are otherwise useful for estimating loads.

SYMBOLS

Measurements were made in U.S. Customary Units. They are presented herein in the International System of Units (SI) with the equivalent values in U.S. Customary Units given parenthetically:

F_A	axial force, N (lb)
F_N	normal force, N (lb)
F_R	resultant force, $\sqrt{F_N^2 + F_A^2}$, N (lb)
h	vertical dimension of the aspect-ratio-6 secondary exhaust nozzle, cm (in.)
l	length of wing surface aft of nozzle, cm (in.)
r	radius of Coanda flap surface, cm (in.)
T	static thrust, N (lb)

T_1	temperature measurement at the thermocouple nearest wing surface, °F
T_2	temperature measurement at the thermocouple farthest from wing surface, °F
V	velocity, m/sec (ft/sec)
x	horizontal projected dimension of Coanda flap, cm (in.)
δ_f	deflection of Coanda flap upper surface at flap trailing edge relative to the wing chord, deg
δ_j	jet-deflection angle, deg
δ_2	deflection angle of second element of double-slotted flap of the wind-tunnel test airplane, deg
η	flap system turning efficiency, F_R/T
USB	upper surface blown jet flap
WCP	wing chord plane

MODEL AND APPARATUS

General Arrangement

The outdoor static test apparatus is illustrated in the photograph of figure 1. The engine used in this series of tests was the United Aircraft of Canada JT-15D-1 turbofan rated at 2,200 pounds of static thrust at sea level standard conditions. This engine has a bypass-ratio of 3.34 and a fan pressure ratio of 1.53. The simulated wing and flap system was of boiler-plate fabrication with the surface contours similar to those of an airplane to be tested in the Langley full-scale tunnel. Details and dimensions of the static test apparatus are given in figure 2. The entire model including the inlet, engine, exhaust nozzles, and wing/flap structure were mounted on a floating frame instrumented to measure both normal and axial forces relative to the engine centerline. Three parts of the model were mounted to the floating frame independently: (1) the inlet was rigidly

mounted to the engine support truss; (2) the engine was mounted on strain gages (at the forward engine mount pivots) which were in turn mounted to the engine support truss; and (3) the wing and flap structures were directly mounted to the floating frame. A rubber seal joined the inlet and the engine fan case, and the secondary nozzle exit was positioned so as not to contact the wing-flap structure. This arrangement permitted direct measurement of thrust loads of the engine-nozzle combination independent of the normal and axial loads determined from the floating frame strain gages. Although tests were conducted with two different inlets (the airplane inlet shown in figure 1 and the bellmouth inlet of figure 2), there was no discernible effect of inlet configuration on the static thrust calibrations.

Exhaust Nozzle Arrangement

The secondary nozzle was a fixed design intended to provide attached flow on the upper surface of the wing-flap system. The secondary nozzle exit was rectangular in shape, had an aspect ratio (width/height) of 6.0, and was canted to provide thrust inclination onto the wing upper surface (about 12° to the wing chord plane). The basic primary nozzle was mounted inside of the secondary nozzle with its circular exit about 1.0 fan diameter upstream of the secondary nozzle exit. During the course of the investigation, the primary nozzle was modified as shown in figure 3. One modification was a simple half-frustum deflector added to the basic round primary nozzle (fig. 3(b)). Another modification was the elliptical exit primary nozzle illustrated in figure 3(c) which had the same exit area as the basic round nozzle.

Wing and Flaps

The wing and flap as shown in figures 1 and 2 were made of boiler plate construction with the wing surface representing the equivalent airplane surface for the wind-tunnel test model. The simulated wing on the test stand was mounted with the chordline set a 0° incidence angle.

45
46
47
48
49
50
51
52

The Coanda flaps were designed to be interchangeable on the wing. These flaps were essentially curved plates configured to fit tangentially the upper-surface contours of a double-slotted flap system designed for the wind-tunnel airplane configuration. The four Coanda flap settings tested, therefore, are related to four selected deflection angles of the double-slotted flaps (flaps nested and $\delta_2 = 20^\circ$, 40° , and 60°). The geometric characteristics of the wing and flaps as related to the secondary nozzle and the wing chord plane are presented in table I. In this investigation the significant flap deflection parameter is the tangency angle at the Coanda flap trailing edge which is defined as δ_f (see sketch at top of table I).

Surface Pressure and Temperature Instrumentation

The wing and flaps were fitted with surface pressure ports and also with surface thermocouples. The locations of the pressure ports are given in figure 4. The locations of the thermocouples are given in figure 5. The pressure ports were connected to a multitube manometer. The thermocouples were connected to a multichannel temperature recorder.

TESTS AND PROCEDURES

The tests were conducted first with the wing and flap removed from the stand in order to calibrate the engine thrust with the aspect-ratio-6 nozzle installed. Although the JT-15D-1 engine is rated at 2,200 pounds static thrust at sea level standard conditions, maximum thrust in this series of tests was limited to 2,000 pounds to avoid gas turbine over-temperature problems resulting from the use of nonoptimized nozzles. A pitot static rake was mounted vertically across the centerline of the exhaust, and the engine was run up to different power settings to calibrate thrust as a function of engine rpm. After the engine thrust was calibrated, the wing and flap were installed and additional runs were made for the range of flap angles given in table I. The forces measured from the strain gages were recorded at the same time a photograph was made of the manometer board that

registered the pressure distribution across the exhaust nozzle and the distribution of the pressure over the wing and flap. Temperatures recorded by the thermocouples were also identified at the same time the force and pressure data were recorded.

RESULTS AND DISCUSSION

The results of the investigation are presented in terms of static turning performance, pressure distributions on the wing and flaps, velocity distribution from the secondary nozzle and velocity profiles of the flow over the wing and flaps, and temperature measurements both on the wing and flap surfaces and in the gas flow from the nozzle exit. The primary variables were flap deflection angle, hot-nozzle modifications, and thrust level. Emphasis has been placed on the extreme condition of maximum thrust (approximately 2,000 pounds) in the presentation of data.

Exhaust Nozzle Flow Characteristics

Characteristics of the efflux at the exit plane of the secondary nozzle were first evaluated with the wing and flap removed. Velocity profiles across the secondary nozzle exit (for an engine thrust of 2,000 pounds) with basic round primary nozzle and with the elliptical primary nozzle (at a thrust of 1,750 pounds) are compared in figure 6. A high velocity region around the middle of the secondary nozzle is apparent with the basic round primary nozzle (fig. 6(a)). This high velocity region was caused to spread laterally when the elliptical primary nozzle was used (fig. 6(b)). Also, the elliptical primary nozzle introduced some distortions in the velocity profiles which are probably related to a slight misalignment of the major ellipse axis with respect to the secondary nozzle axis. Similar velocity profile data are not available for the round primary nozzle with the deflector.

A comparison of the temperature patterns of the flow at the exit nozzle plane with the basic round primary nozzle and with the elliptical primary

nozzle are presented in figure 7 for a thrust of 2,000 pounds and 1,750 pounds, respectively. Temperatures were measured at two heights above the location at which the wing upper surface was to be positioned: $h = 4.68$ cm (1.685 in.) and 11.58 cm (4.560 in.). With the round primary nozzle, peak temperatures of the order of $1,000^{\circ}\text{F}$ occurred along the centerline and were not greatly different at the two vertical heights (fig. 7(a)). With the elliptical primary nozzle, there was considerable spanwise distortion of the temperature patterns at the two vertical heights and the peak temperatures of the order of 700°F did not necessarily occur on the nozzle centerline (fig. 7(b)). This distortion of the temperature pattern with the elliptical primary nozzle is probably related to the previously mentioned misalignment of the major ellipse axis relative to the secondary nozzle axis. The main point of these results is the general lowering of the peak temperatures from the order of $1,000^{\circ}\text{F}$ to the order of 700°F by changing from a round primary nozzle to an elliptical primary nozzle.

Temperature data were obtained only at the secondary nozzle centerline with the round primary nozzle equipped with the deflector and these results are compared with similar data with the basic round primary nozzle in figure 8. Temperatures at the two vertical heights were essentially equal and of the order of $1,000^{\circ}\text{F}$ with the basic round primary nozzle (fig. 8(a)). With the deflector on the round primary nozzle, the temperature at the measuring points nearest the wing surface location dropped to about 460°F whereas the temperatures at the measuring point away from the wing surface location increased to about $1,100^{\circ}\text{F}$ (fig. 8(b)). Use of the deflector on the primary nozzle should therefore be effective in reducing temperatures on the wing surface.

Static Turning Characteristics

The effectiveness of an upper-surface blown jet flap in forward flight is dependent to a large degree on how well the engine efflux attaches to the deflected upper surface of the wing and flap and the efficiency of turning the jet sheet, and consequently, the thrust vector, in terms of

thrust recovery at the deflected thrust condition. Static turning tests were made, therefore, to determine these characteristics as functions of the engine primary nozzle geometry, trailing-edge flap angle, and engine thrust level. For each configuration tested, the engine static thrust was determined as a function of fan rpm with the wing surface and flap removed. Although some of these tests were conducted with a nacelle inlet designed for the large-scale wind-tunnel model and others were conducted with a bell-mouth inlet, there was no discernible effect of inlet configuration on the static thrust calibrations.

The results of the static turning tests are presented in figure 9. The static turning performance is presented in terms of the jet turning angle, δ_j , and the flap turning efficiency, η (which is a measure of the static thrust recovery at the jet turning angle achieved). Both the flap deflection angle, δ_f , and the jet turning angle, δ_j , are referenced to the wing chord plane which was parallel with the engine centerline. The flap deflection angle, δ_f , is defined as the deflection of the upper-surface tangency line at the flap trailing edge with respect to the wing chord plane. Thus, for the clean configuration corresponding to the basic airfoil upper surface, the upper-surface tangency angle, δ_f , was 9.2° . The aspect-ratio-6.0 secondary nozzle was configured to direct the jet sheet onto the upper surface of the wing at an angle of 11.75° with respect to the engine centerline. This thrust axis inclination was confirmed experimentally during engine thrust calibrations with the wing and flap removed (see fig. 9(a)).

Effect of primary nozzle geometry. - Static turning tests were originally conducted with a standard primary nozzle having a round exit. As shown in figure 9(a), tests conducted with this round primary nozzle for the $\delta_f = 70^\circ$ configuration provided fairly good static turning performance at a very high efficiency ($\delta_j = 58^\circ$ and $\eta = 0.97$). This round primary nozzle, however, caused a high temperature problem on the wing upper surface and on the knee of the Coanda flap due to direct impingement of the hot-core flow. Therefore, the primary nozzle had to be modified to relieve the

temperature problem. Tests were conducted with a deflector on the primary nozzle exit designed to divert the hot-core flow off of the wing upper surface (see fig. 3). As shown in figure 9(a), when this deflector was used on the round primary nozzle with the same flap deflection angle ($\delta_f = 70^\circ$), the static turning performance suffered appreciably ($\delta_j = 51^\circ$ and $\eta = 0.83$). This loss in turning effectiveness and flap turning efficiency is attributed to turbulence created by the deflector and to reduction of the impingement angle onto the wing upper surface. The engine was then fitted with a modified primary nozzle having an elliptical exit as illustrated in figure 3. This nozzle was designed to spread the hot-core flow inside the aspect-ratio-6.0 secondary nozzle for the purpose of relieving the temperature problem without actually diverting the hot-core flow off of the wing surface. As shown in figure 9(a), static turning tests conducted with the elliptical primary nozzle and with the same flap deflection angle ($\delta_f = 70^\circ$) provided static turning performance much better than that obtained with the deflector on the round nozzle and almost as good as that obtained with the original round primary nozzle ($\delta_j = 55^\circ$ and $\eta = 0.93$). As will be shown in a subsequent section, this elliptical primary nozzle also provided the required temperature relief on the upper surface of the wing and flap.

Effect of trailing-edge flap deflection.- Static turning tests were conducted over the range of flap deflections only for the configuration which utilized the deflector on the round primary nozzle and the results are presented in figure 9(b). (Similar tests are planned for the configuration utilizing the elliptical primary nozzle in view of its improved performance cited in the previous section.) The results shown in figure 9(b) indicate reasonably good static turning performance for all flap deflections except $\delta_f = 70^\circ$ (turning angle losses ranged from 2° to 8° and η was greater than 0.90). By inference static turning performance with the elliptical primary nozzle should at least equal those obtained with the deflector on the primary nozzle over the lower range of flap deflections.

Effect of thrust level.- The static turning performance as a function of thrust level for the $\delta_f = 70^\circ$ condition and for both the round primary nozzle equipped with the deflector and the elliptical primary nozzle are presented in figure 9(c). These results indicate considerably less dispersion over the thrust range for the tests conducted with the elliptical primary nozzle for which the turning performance was reasonably good over the range of thrusts tested ($\delta_j \approx 55^\circ$ and $\eta \approx 0.93$) than with the round primary nozzle with the deflector.

Flow Characteristics With Wing and Flaps Installed

During the tests to determine the static turning characteristics, measurements were also made to evaluate surface pressures and temperatures on the wing and flaps, and flow velocities and temperatures in the region above the wing-flap surface. As mentioned previously, the objective of this investigation was to determine an acceptable compromise between static turning performance and the surface temperature constraints on the wing and flaps. The following sections describe the wing-flap environment as functions of modifications of the primary nozzle.

Surface pressures and temperatures.- The results of surface pressure measurements on the wing and flaps aft of the aspect-ratio-6.0 secondary nozzle are presented in figures 10 and 11 and the results of corresponding surface temperature measurements are presented in figures 12 through 14. These results will be discussed together where applicable.

With the basic round primary nozzle and for the 70° flap deflection the surface pressure data are shown in figure 10 and the corresponding surface temperature data are shown in figure 12. The pressure data are presented as chordwise pressure profiles with leaders directed from each pressure port. Arrowheads on the leaders indicate pressure direction (down for positive pressure on the surface and up for negative or suction pressure on the surface), and the length of the leaders reflect the magnitude of individual pressures. The results shown in figure 10 provide a good indication of attached flow well back toward the trailing edge of the

70° deflected upper surface. Also, suction pressures are generated forward of the flap on the wing surface except directly on the centerline where positive pressures occurred due to jet impingement. The high-temperature problem on the wing and flap surface (fig. 12) is associated with the impingement of the hot primary flow from the basic round nozzle. Temperatures of the order of 800°F were measured just forward of the flap.

In order to relieve the surface temperature problem, the deflector shown in figure 3 was installed on the primary nozzle. Surface pressure data obtained with this modification are presented in figure 11 and corresponding surface temperature data are presented in figure 13 through the range of flap angles tested. The data of figures 11(d) and 13(d) are for the flap deflection of 70° and are therefore pertinent for direct comparison with the previously discussed results for the basic round primary nozzle. The deflector on the primary nozzle caused the hot-core flow to be deflected away from the wing surface so that maximum surface temperatures were under 400°F or less than half those obtained with the basic round primary nozzle (compare figs. 12 and 13(d)). The corresponding surface pressure data of figure 11(d) obtained with the deflector on the primary nozzle are not appreciably different from that obtained with the basic round primary nozzle (fig. 10).

As pointed out in the section on static turning characteristics, the use of the deflector on the primary nozzle resulted in unacceptable turning losses and, therefore, the primary nozzle was modified to the elliptical exit shown in figure 3 in an effort to spread the hot-core flow laterally inside the aspect-ratio-6.0 secondary nozzle. Surface temperature results obtained with this elliptical primary nozzle and for the 70° flap deflection are presented in figure 14 which indicates maximum temperatures just forward of the flap of the order of 500°F, or about 300°F lower than with the basic round nozzle. These 500°F surface temperatures were deemed acceptable for the stainless steel skin and thermal insulation blanket to be utilized on the wind-tunnel model. This factor in conjunction with the acceptable static turning performance caused the elliptical primary nozzle to be selected for the wind-tunnel model.

Flow characteristics above wing and flaps.- Sample results of the gas temperature profiles along the nozzle centerline in the flow region above the wing and flap are presented in figure 15. Corresponding velocity profiles are presented in figure 16. These data were obtained with the basic round primary nozzle and with $\delta_f = 70^\circ$ at 2,000 pounds of thrust. In general, the gas temperatures above the flap surface are considerably lower than the corresponding surface temperatures which indicate the high-temperature core flow tends to adhere to the flap surface. The velocity profiles (fig. 16) indicate a rather rapid decay in average velocity as the flow progresses toward the flap trailing edge and a dissipation of energy as the exhaust flow mixes with entrained ambient air. The most important point is that peak velocities of the order of 460 m/sec (1,400 ft/sec) at the secondary nozzle exit decayed to the order of 164 m/sec (500 ft/sec) at the flap trailing edge. This rapid decay of peak velocity is probably related to the rapid mixing of the engine efflux with ambient air as evidenced by the attendant decay in temperature.

CONCLUDING REMARKS

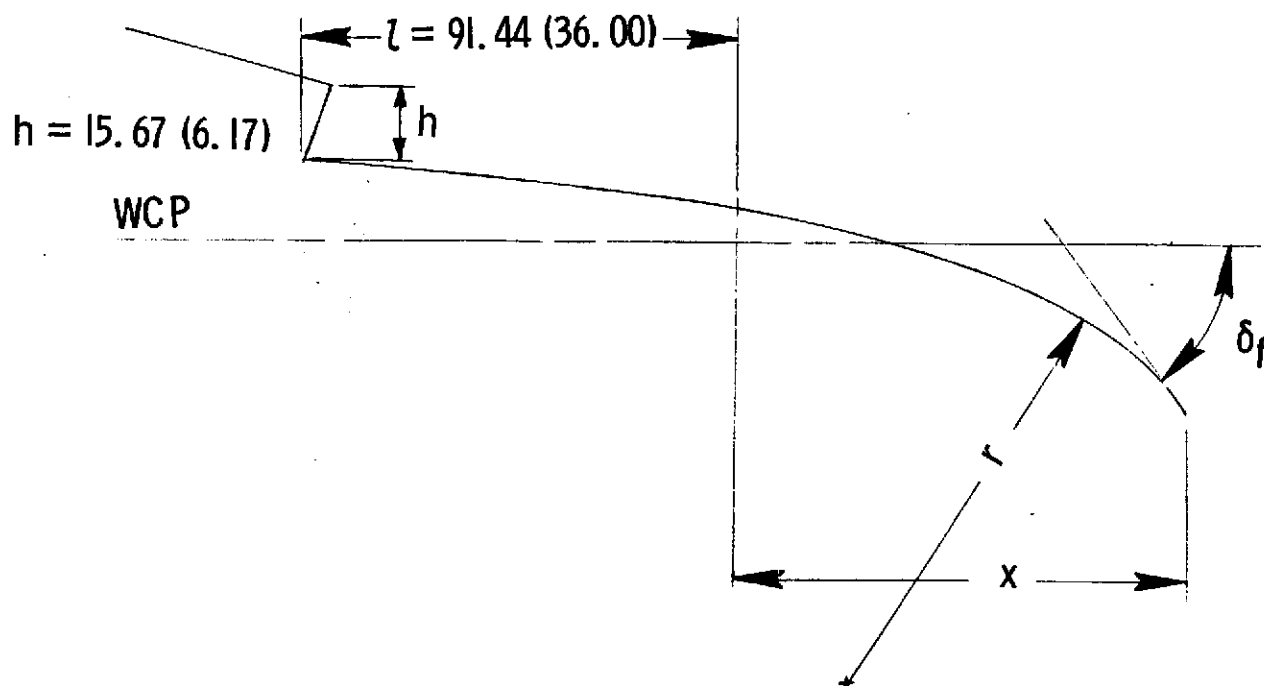
An investigation to establish the static turning performance and flow environmental factors of a specifically designed upper-surface blown jet-flap configuration utilizing a full-scale turbofan engine propulsion system led to the following results:

1. Acceptable surface temperature conditions on the wing and flap were obtained with either the elliptical primary nozzle or the round primary nozzle fitted with a deflector to divert the hot-core flow away from the wing surface, but unacceptable surface temperatures occurred on the wing with the basic round primary nozzle.

2. Acceptable static turning performance was obtained with either a circular or elliptical primary nozzle inside of the rectangular aspect-ratio-6.0 secondary nozzle, but unacceptable static turning performance resulted at the 70° flap angle when a deflector was used on the round primary nozzle.

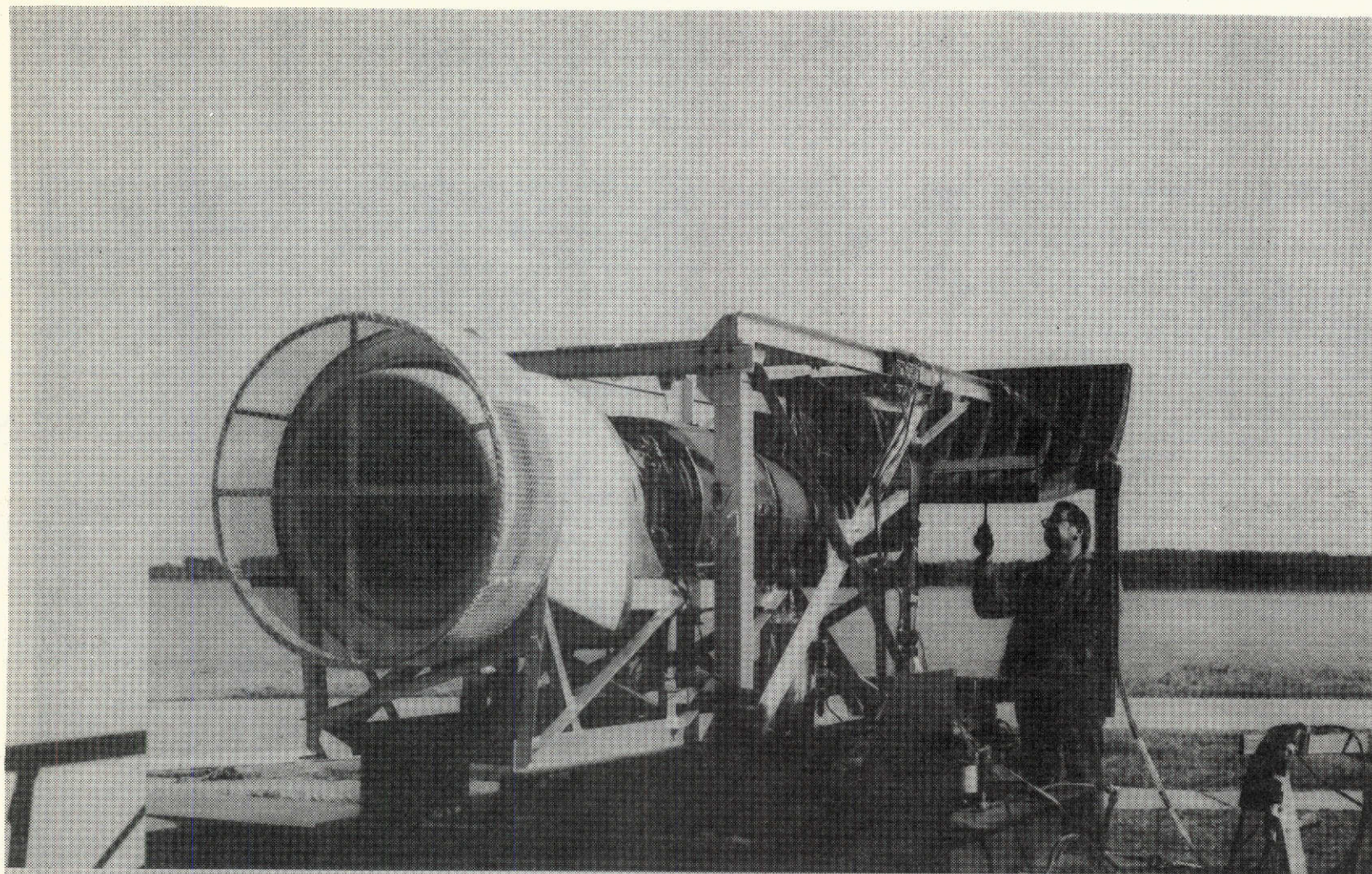
3. For the maximum thrust condition and with the largest flap deflection angle investigated, peak velocities of the order of 460 m/sec (1,400 ft/sec) at the secondary nozzle exit decayed to about 164 m/sec (500 ft/sec) at the flap trailing edge.

TABLE I.- GEOMETRIC CHARACTERISTICS OF WING AND FLAPS



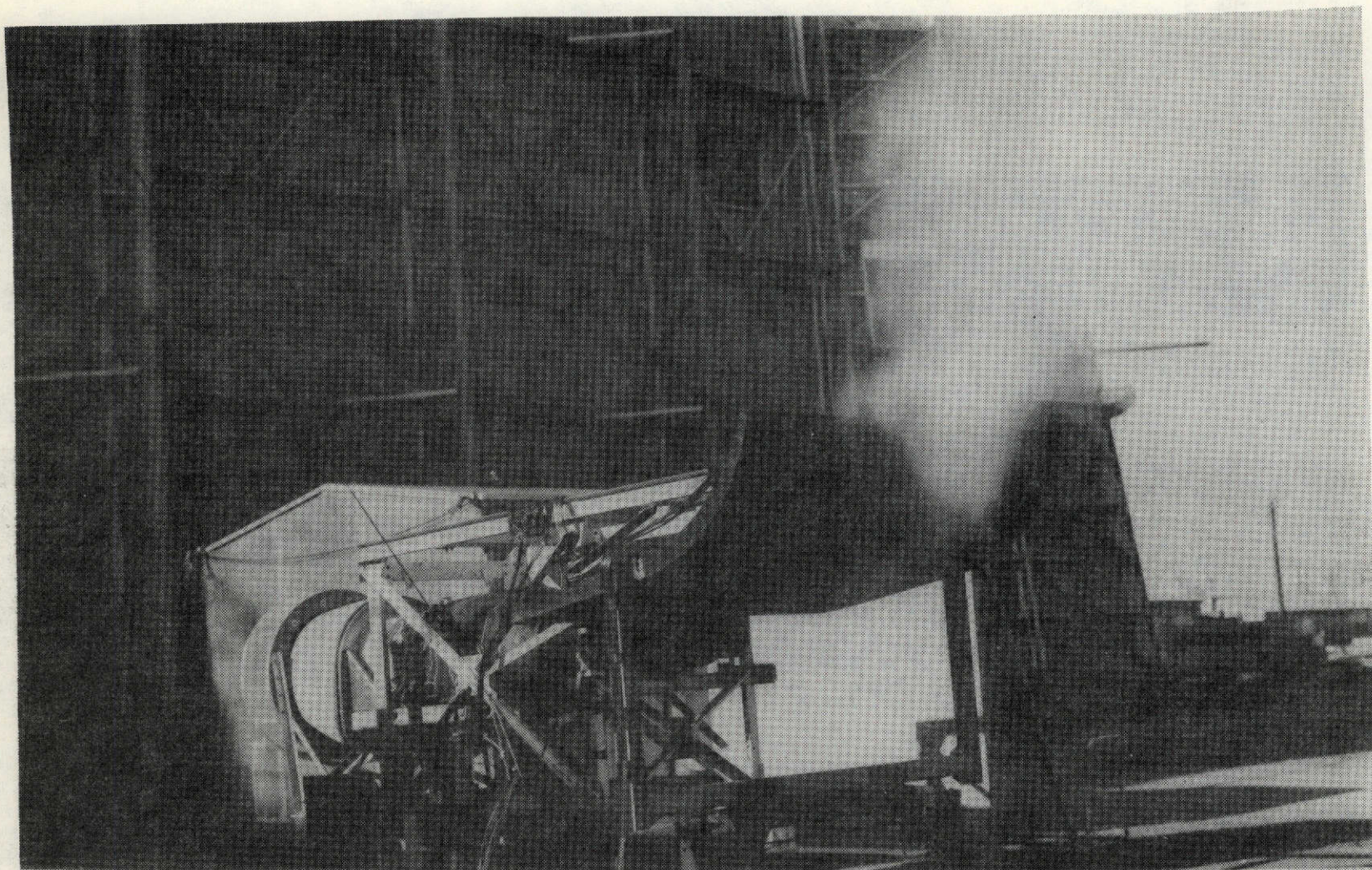
Flap Configuration	δ_f , deg	r , cm (in.)	x , cm (in.)
Retracted	9.2		56.52 (22.25)
Extended $\delta_2 = 20^\circ$	29.8	124.46 (49.00)	99.06 (39.00)
Extended $\delta_2 = 40^\circ$	50.8	92.08 (36.25)	93.47 (36.80)
Extended $\delta_2 = 60^\circ$	70.0	79.38 (31.25)	79.29 (31.20)

Note: δ_2 refers to the nominal deflection with respect to the wing chord plane of the second chordwise element of a double-slotted flap designed for the wind-tunnel airplane configuration.



(A) THREE QUARTER FRONT VIEW

FIGURE 1.- OUTDOOR STATIC TEST APPARATUS WITH AIRPLANE INLET, JT15D-1 TURBOFAN ENGINE, ASPECT-RATIO 6.0 SECONDARY NOZZLE AND SIMULATED USB WING AND FLAP.



(6) THREE-QUARTER REAR VIEW WITH SMOKE TO SHOW TURNING FLOW.

FIGURE 1.- CONCLUDED.

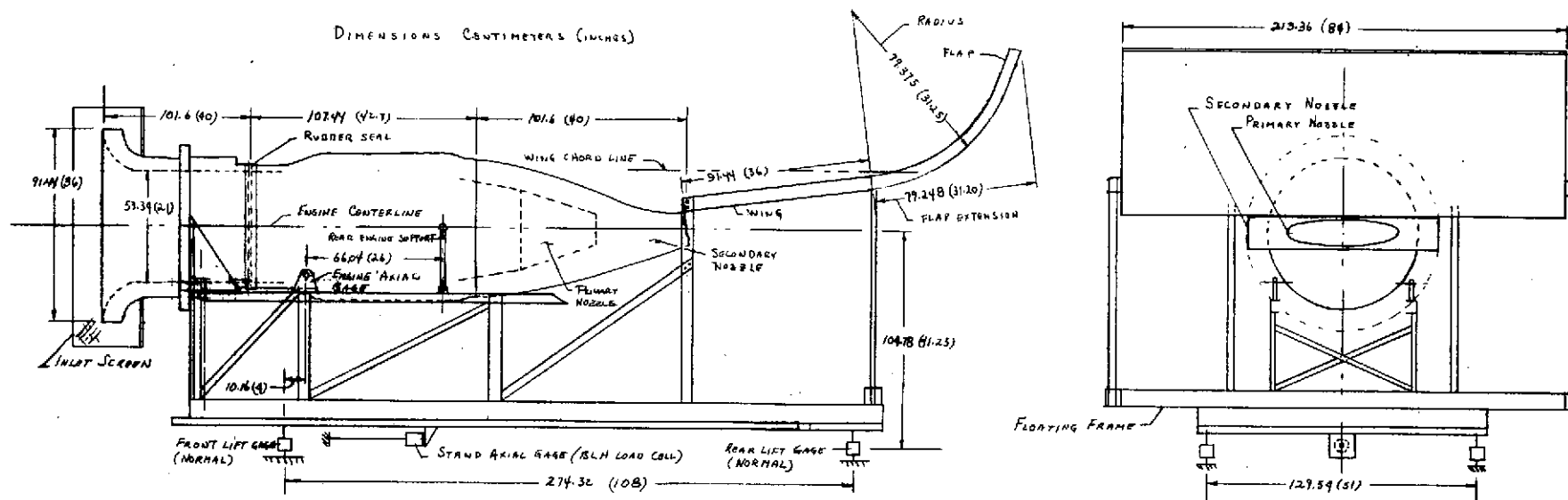
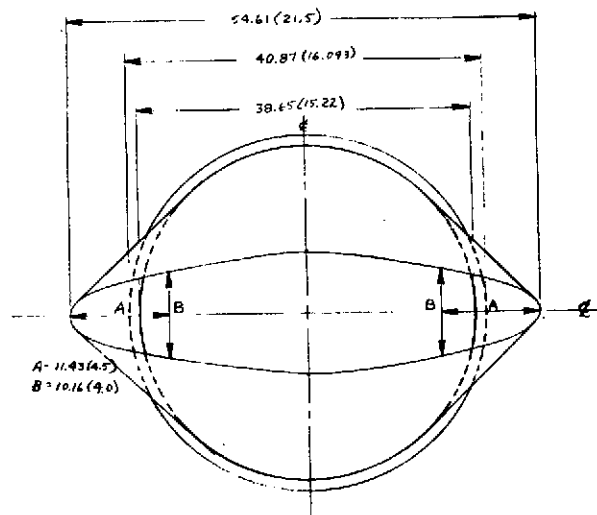
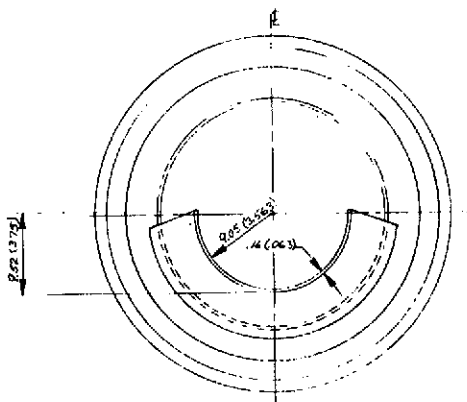
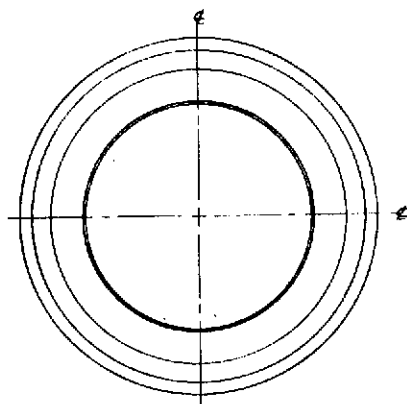
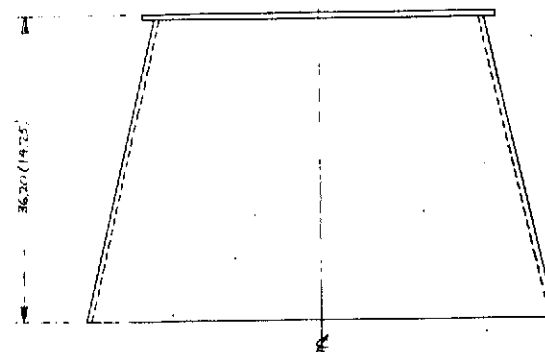
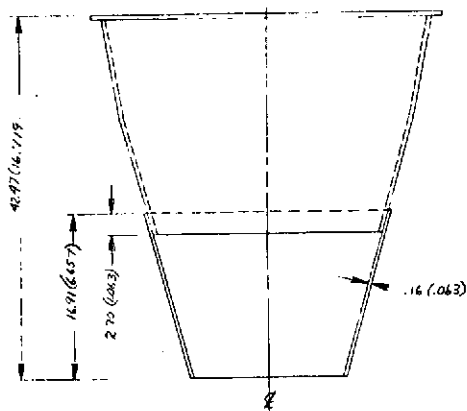
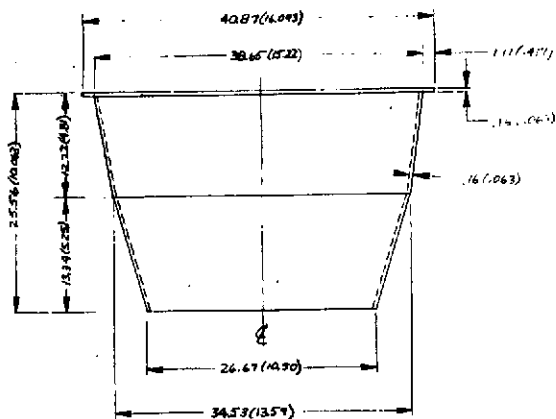


FIGURE 2. SKETCH OF STATIC TEST APPARATUS.



(a) ROUND NOZZLE

(b) ROUND NOZZLE WITH DEFLECTOR

(c) ELLIPTICAL NOZZLE

FIGURE 3.- SKETCH OF PRIMARY NOZZLES. DIMENSIONS CM. (IN.)

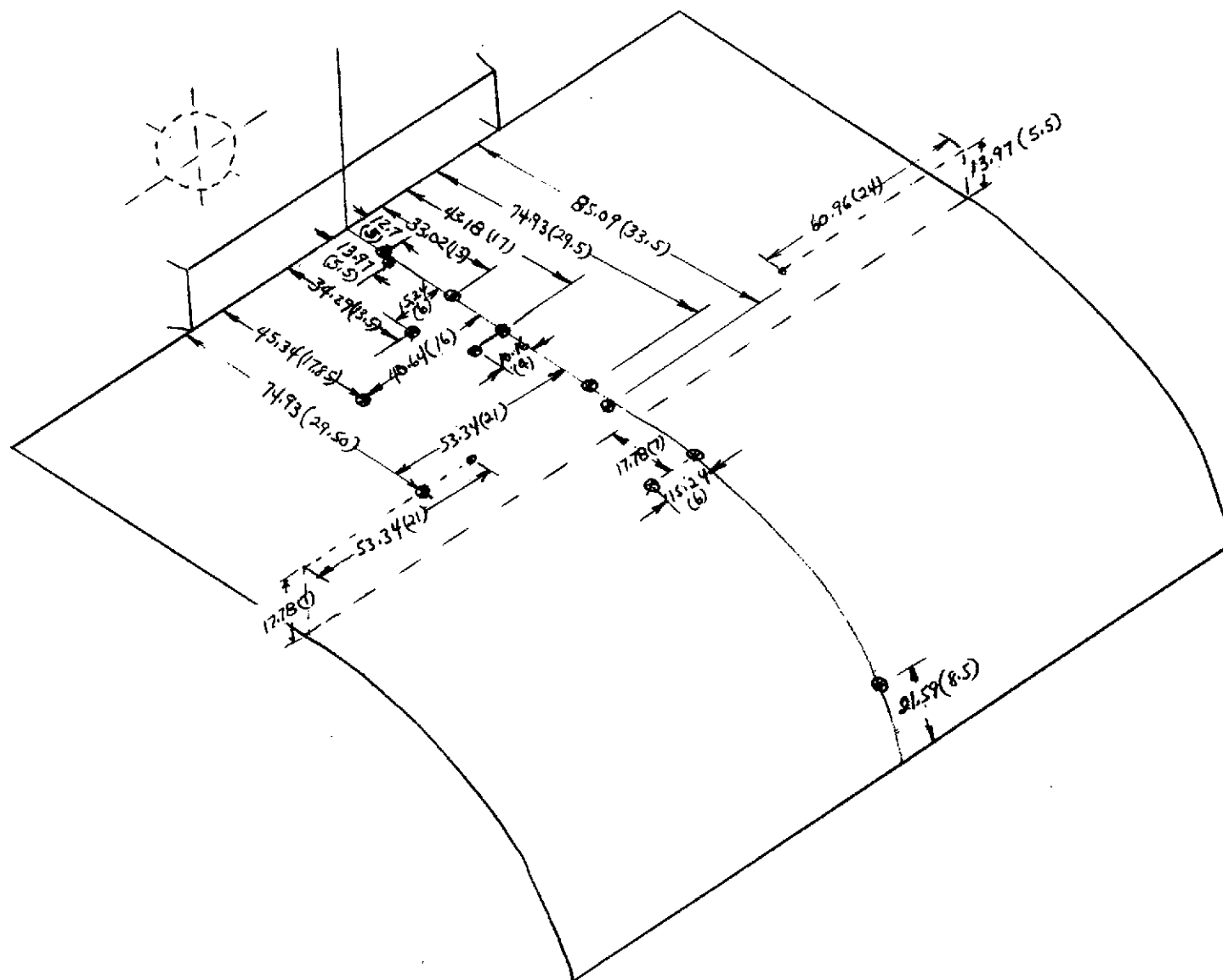
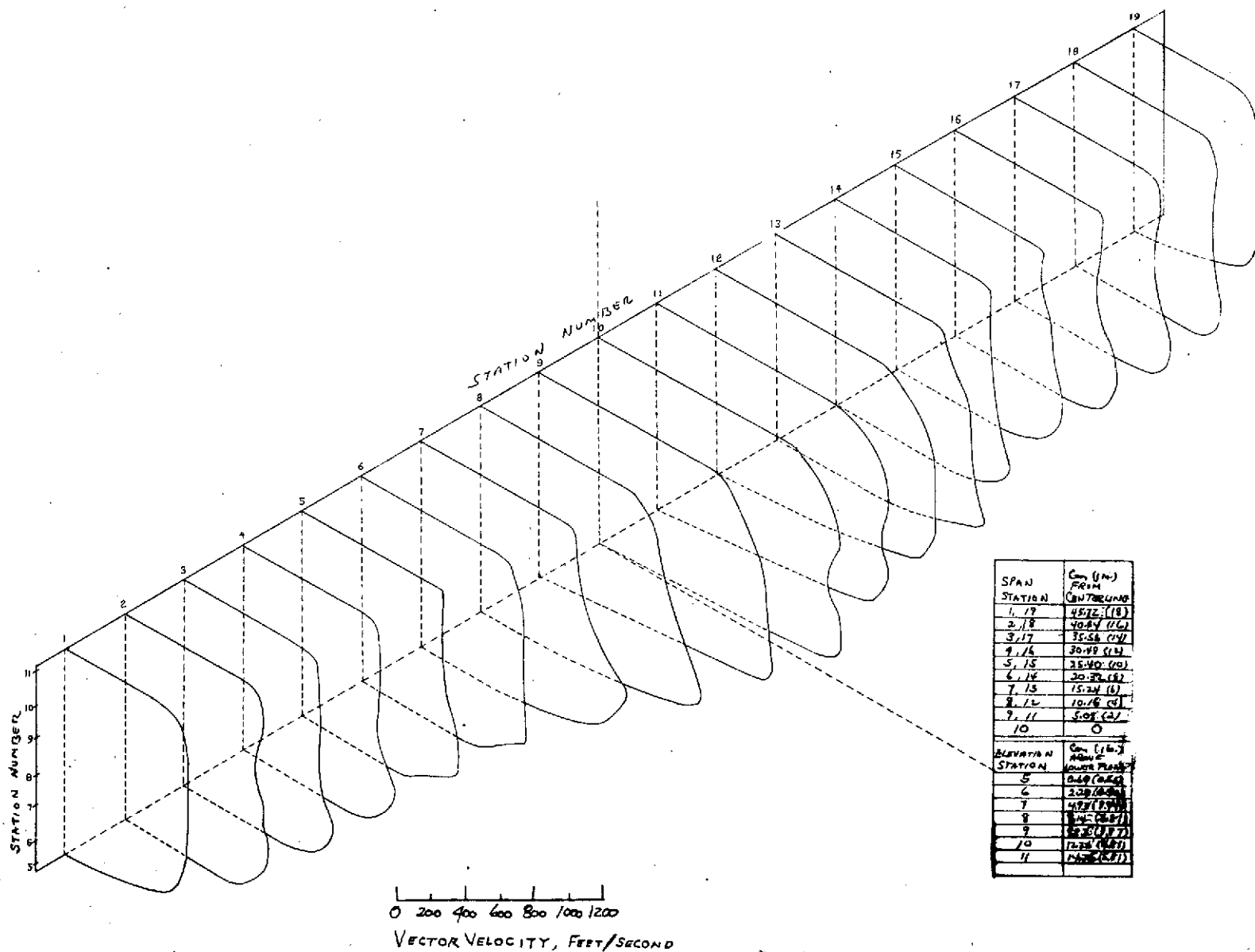
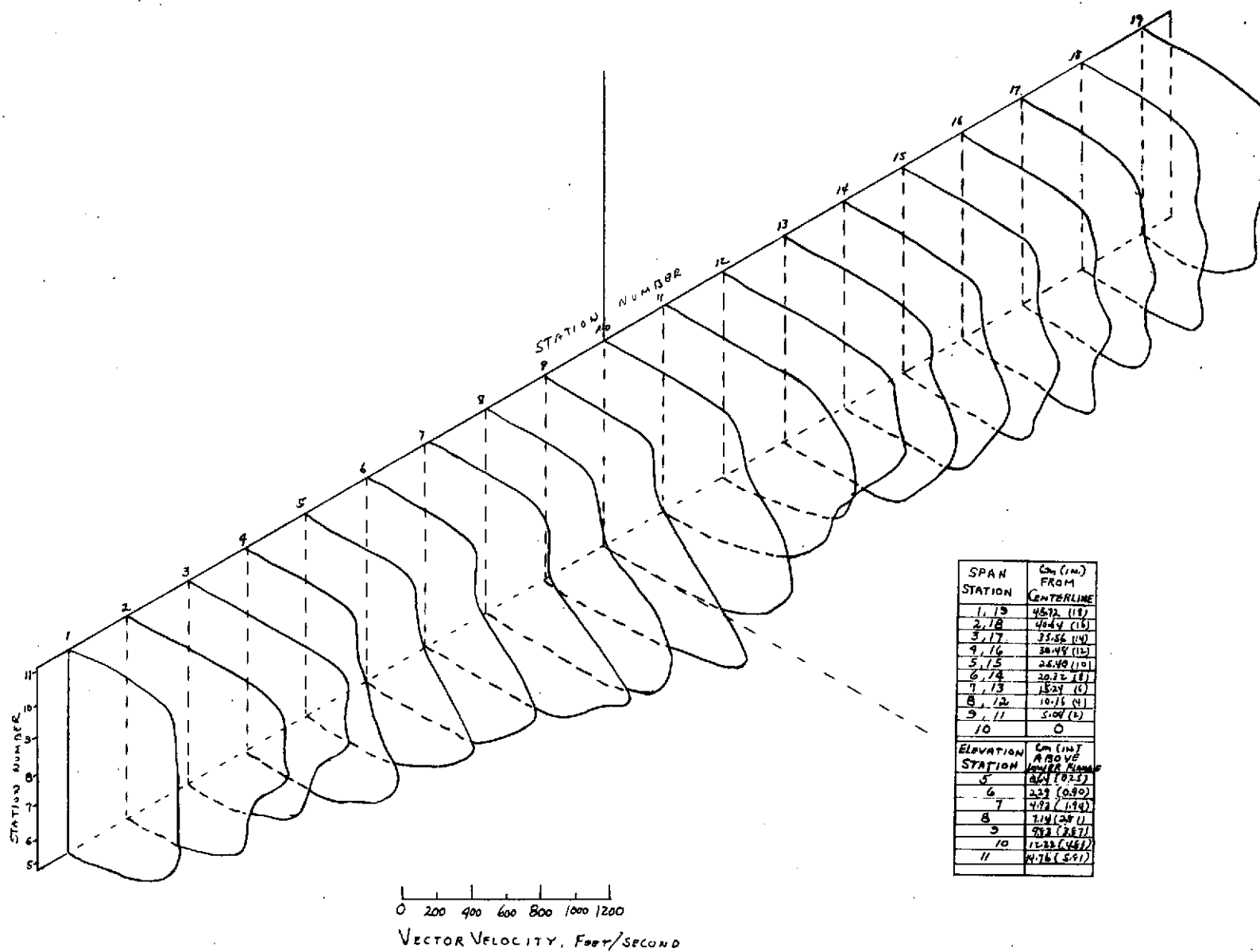


FIGURE 5 - THERMOCOUPLE LOCATION ON WING AND FLAP. ALL DIMENSIONS CM (IN) . $\delta_f = 70^\circ$.



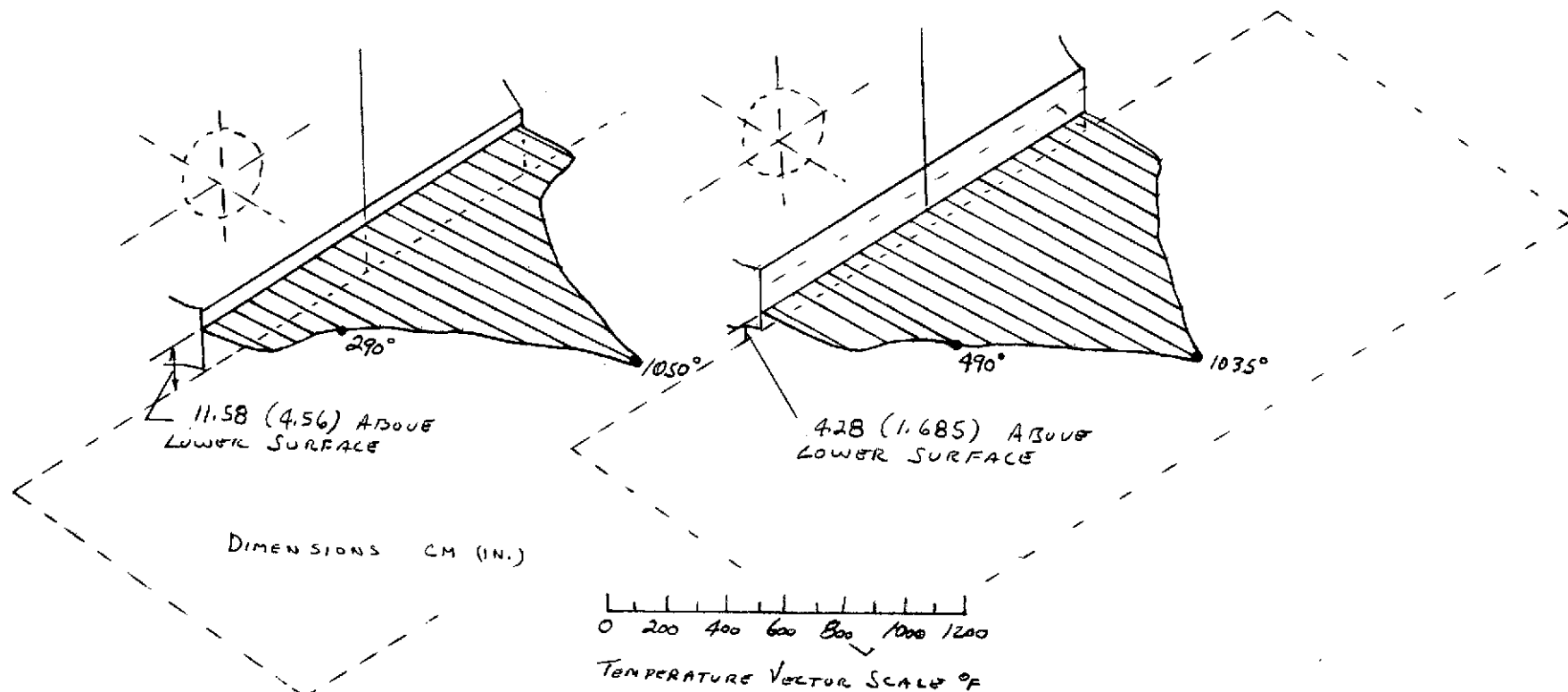
(a) WITH BASIC ROUND PRIMARY NOZZLE, $T = 2000^\circ \text{R}$ (100%)

FIGURE 6 - VELOCITY PROFILE ACROSS THE SECONDARY EXHAUST NOZZLE.



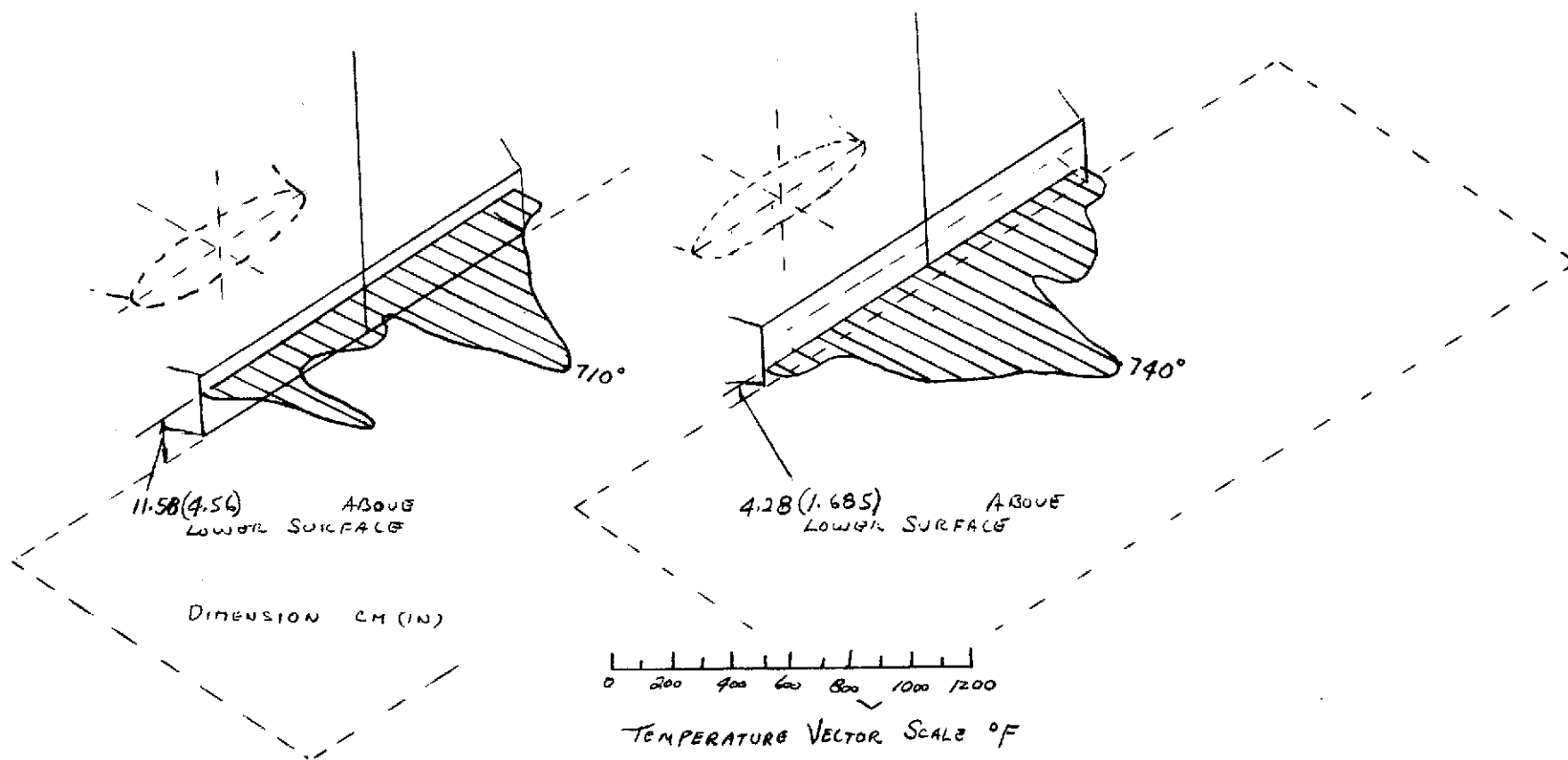
(b) With elliptical primary nozzle; $T=1750$ lbs. (87.5%)

FIGURE 6 -- CONCLUDED.



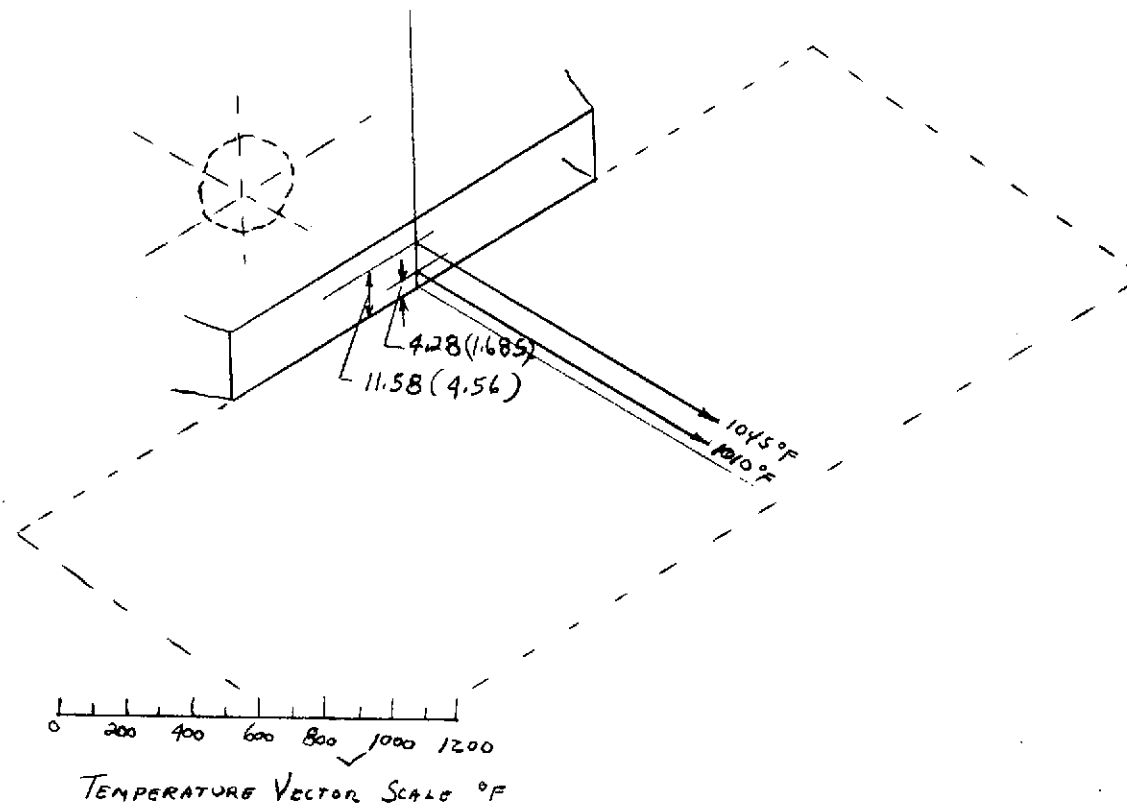
(a) With basic round primary nozzle;
 $T = 2000$ lbs. (100%)

FIGURE 7 - TEMPERATURE PROFILE OF EXHAUST GAS EFFLUX ACROSS THE EXIT OF THE SECONDARY NOZZLE.



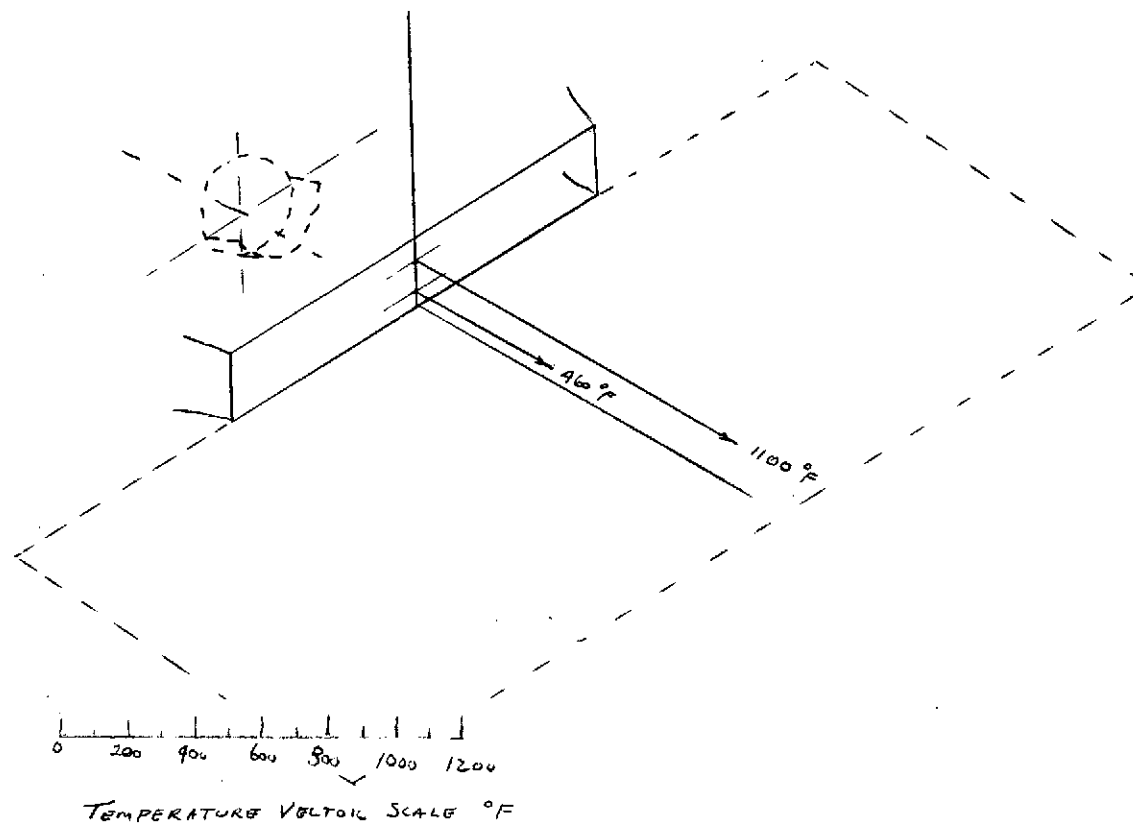
(b) With elliptical primary nozzles;
 $T = 1750$ lbs. (87.5%)

FIGURE 7 .. CONCLUDED.



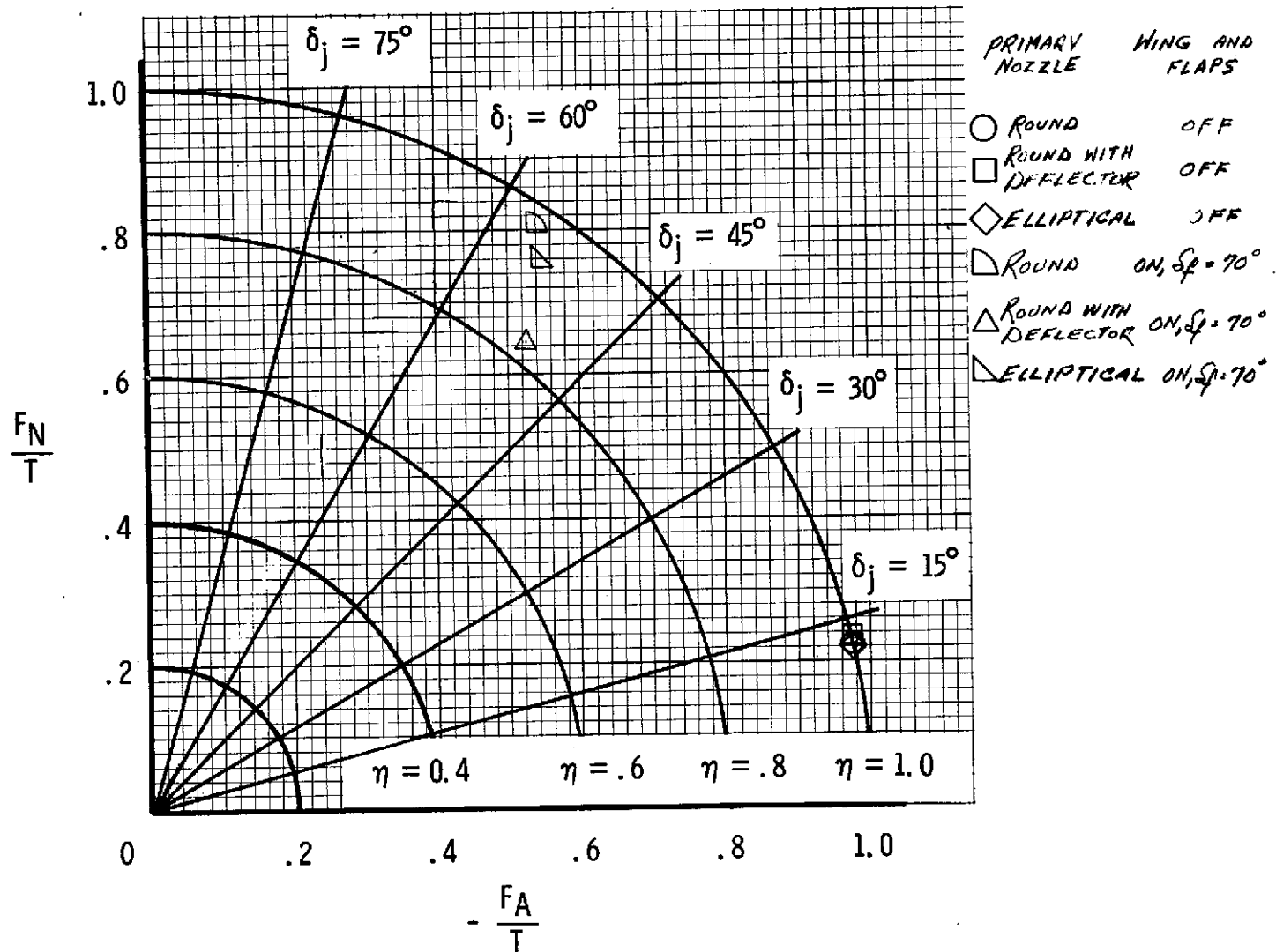
(a) With basic round primary nozzle;
 $T = 2000$ lbs. (100%)

FIGURE 8 -- TEMPERATURE OF EXHAUST GASEFFLUX AT EXHAUST EXIT CENTERLINE.
 DIMENSIONS ARE IN CENTIMETERS (INCHES).



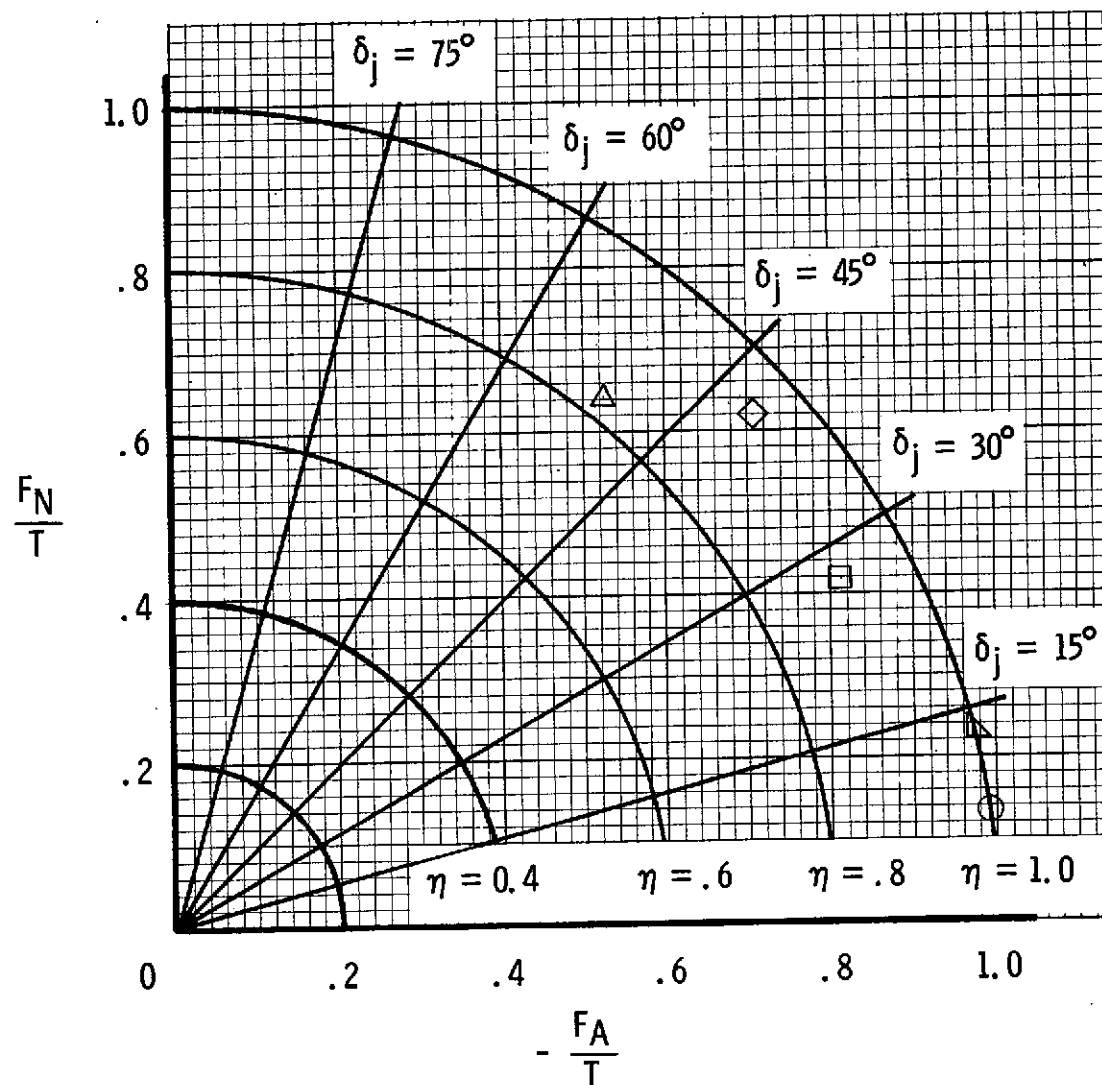
(b) With deflector on round primary nozzle;
 $T = 2000$ lbs (100 %)

FIGURE 8 - CONCLUDED.



(a) Effect of primary nozzle modifications; $T = 2000$ lbs.

Figure 9.- static turning performance.

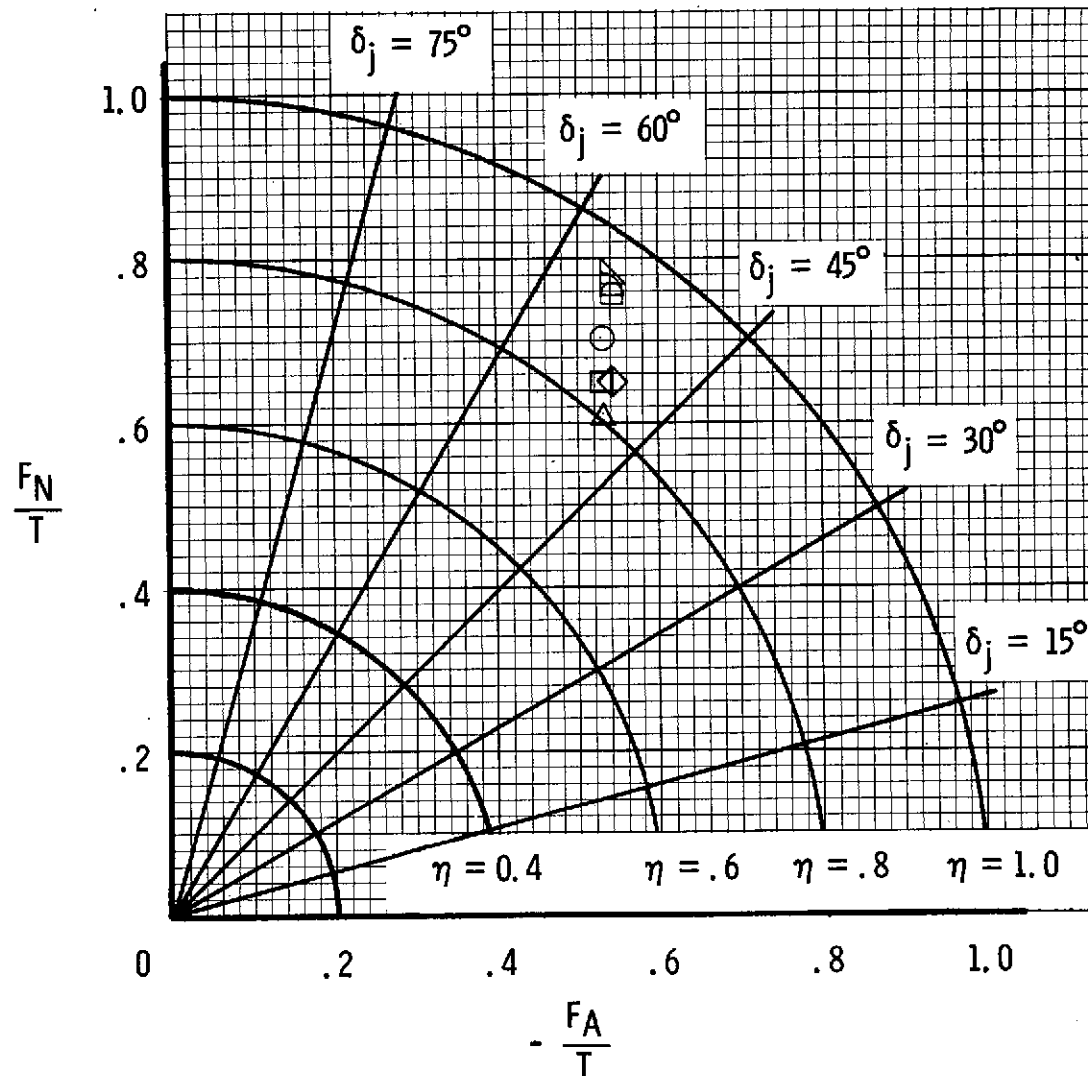


(b) Effect of flap deflection; round primary nozzle with deflector.
Figure 9. - Continued.

Round nozzle with deflector,

$\delta_j = 70^\circ$ THRUST, lbs.

- 260
- 700
- ◇ 1360
- △ 1960



$\delta_j = 70^\circ$ ELLIPTICAL NOZZLE

THRUST, lbs.
280

- △ 1240
- ◻ 2000

(c) Effect of Thrust

Figure 9.- Concluded.

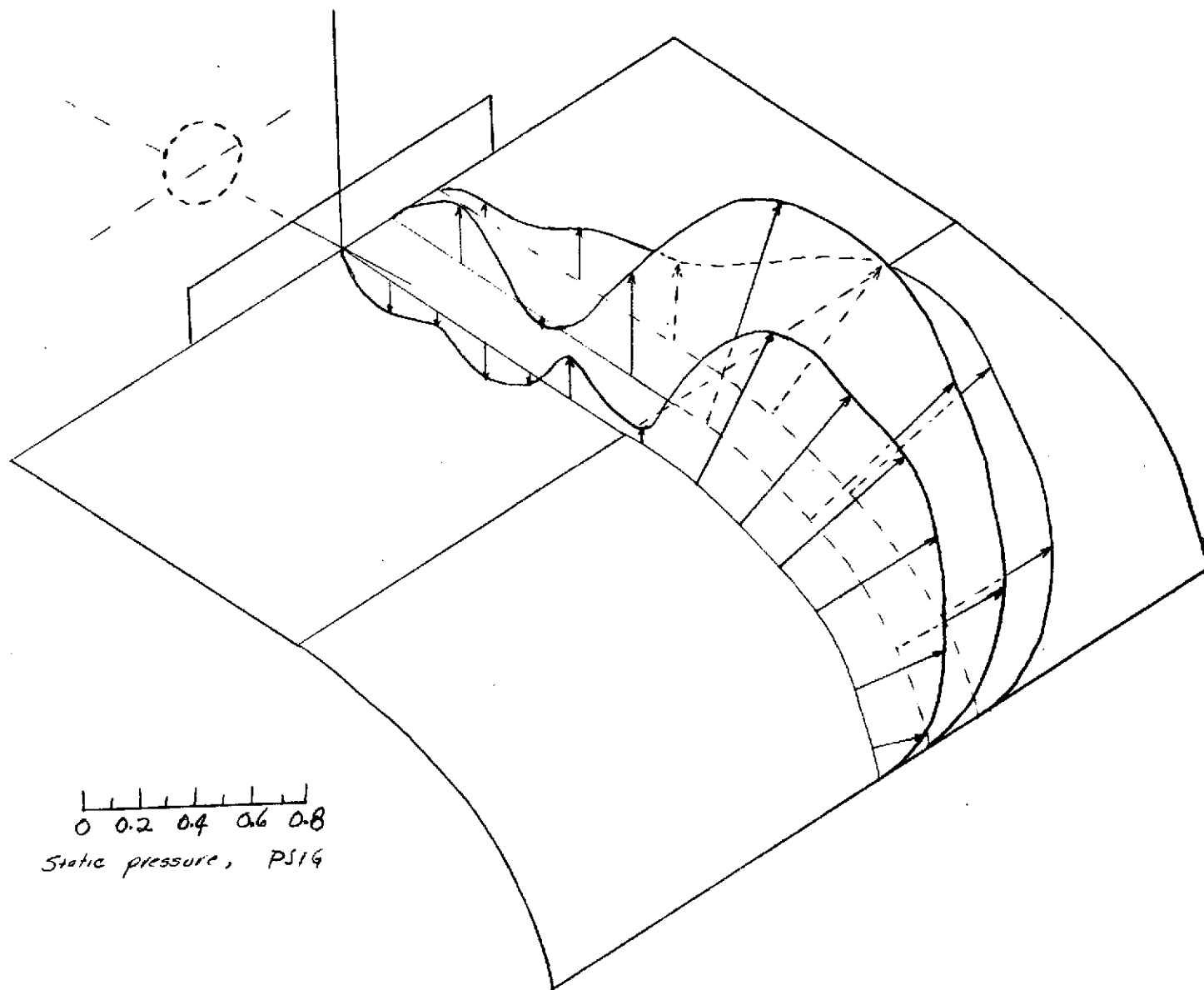
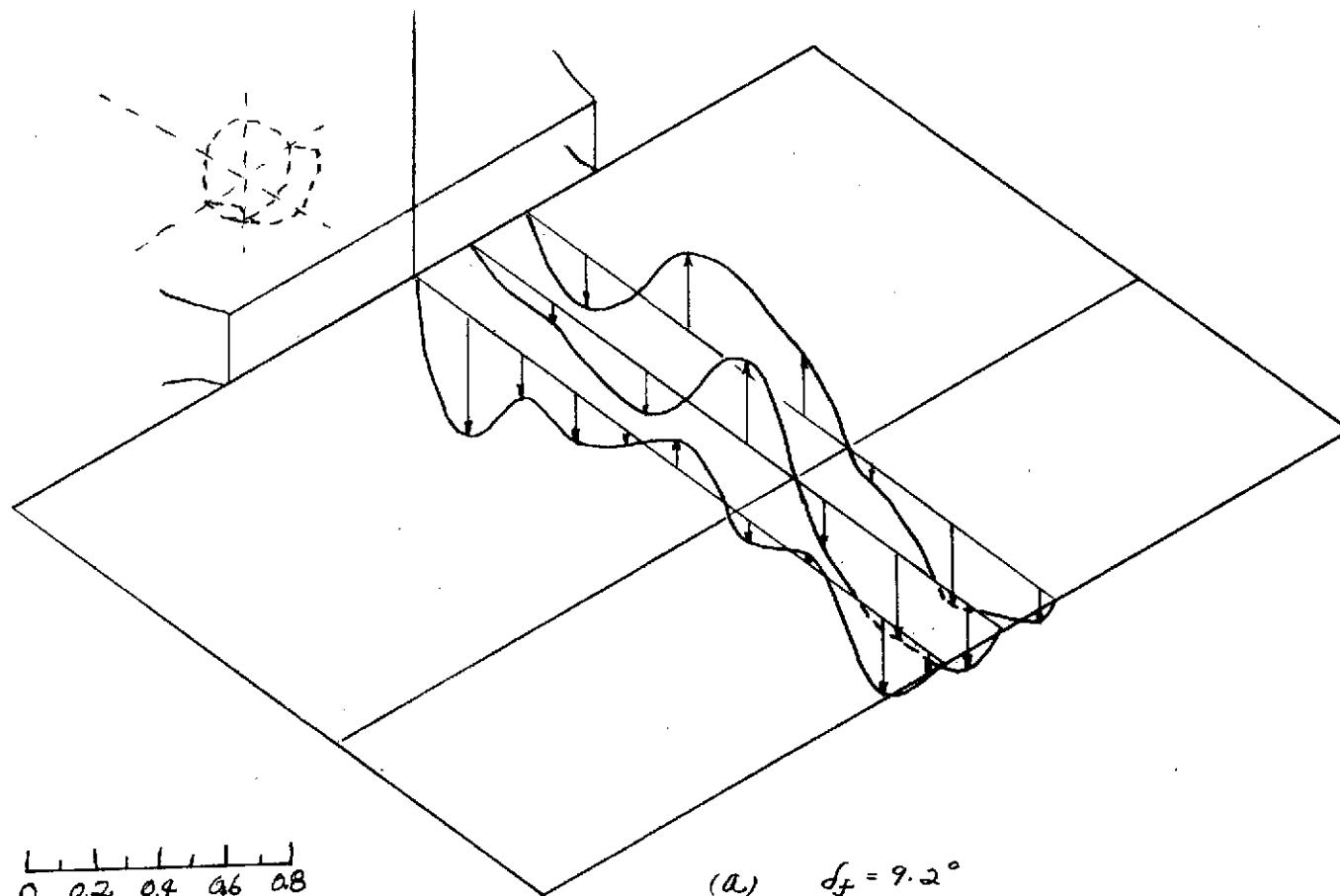
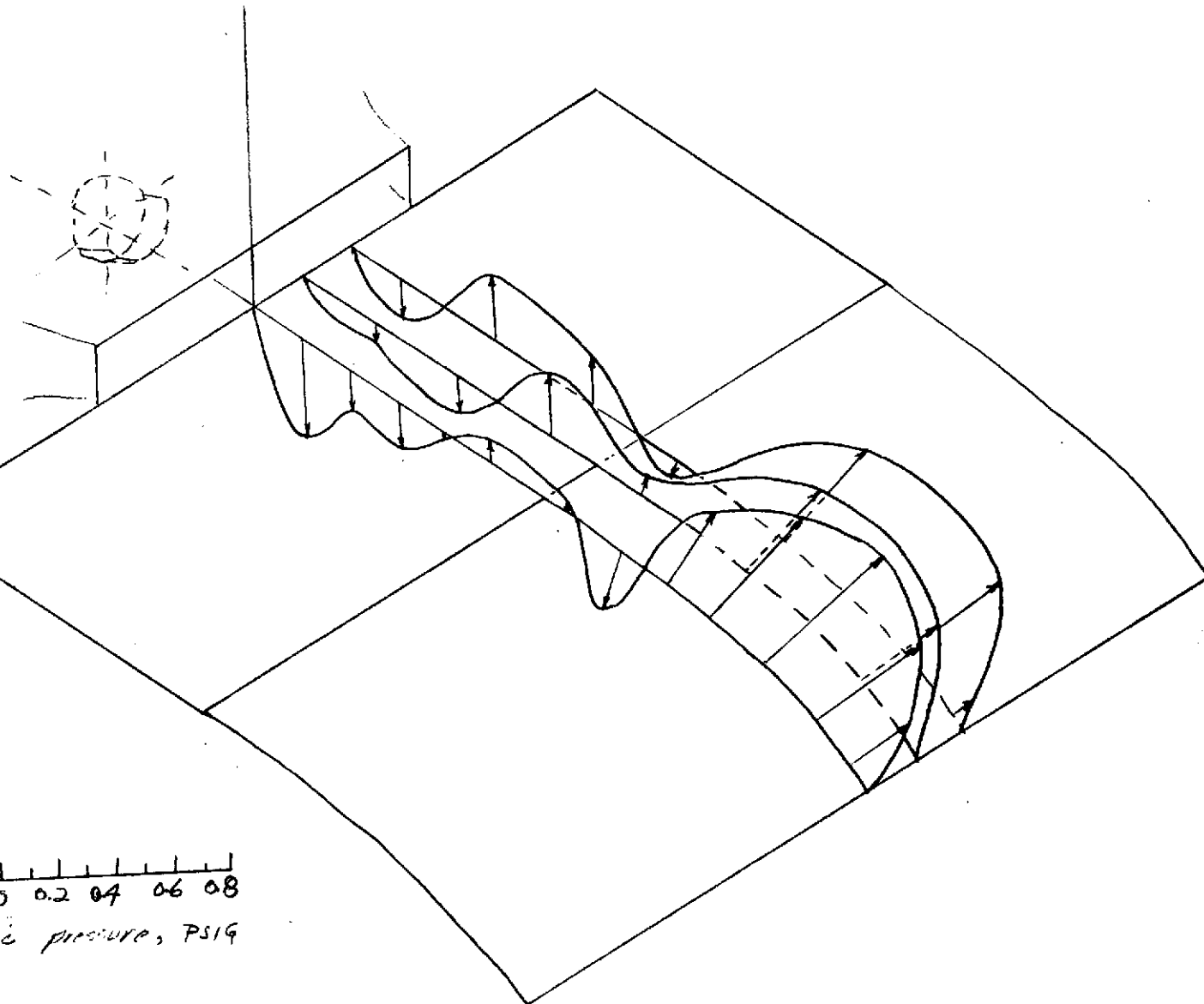


FIGURE 10 -- PRESSURE DISTRIBUTION OVER WING AND FLAP. BASIC ROUND PRIMARY,
2000 lbs THRUST. $\delta_f = 70^\circ$.



0 0.2 0.4 0.6 0.8
Static pressure PSIG

FIGURE 11 -- PRESSURE DISTRIBUTION OVER WING AND FLAP. Round primary nozzle with deflector; 1920 lbs. THRUST

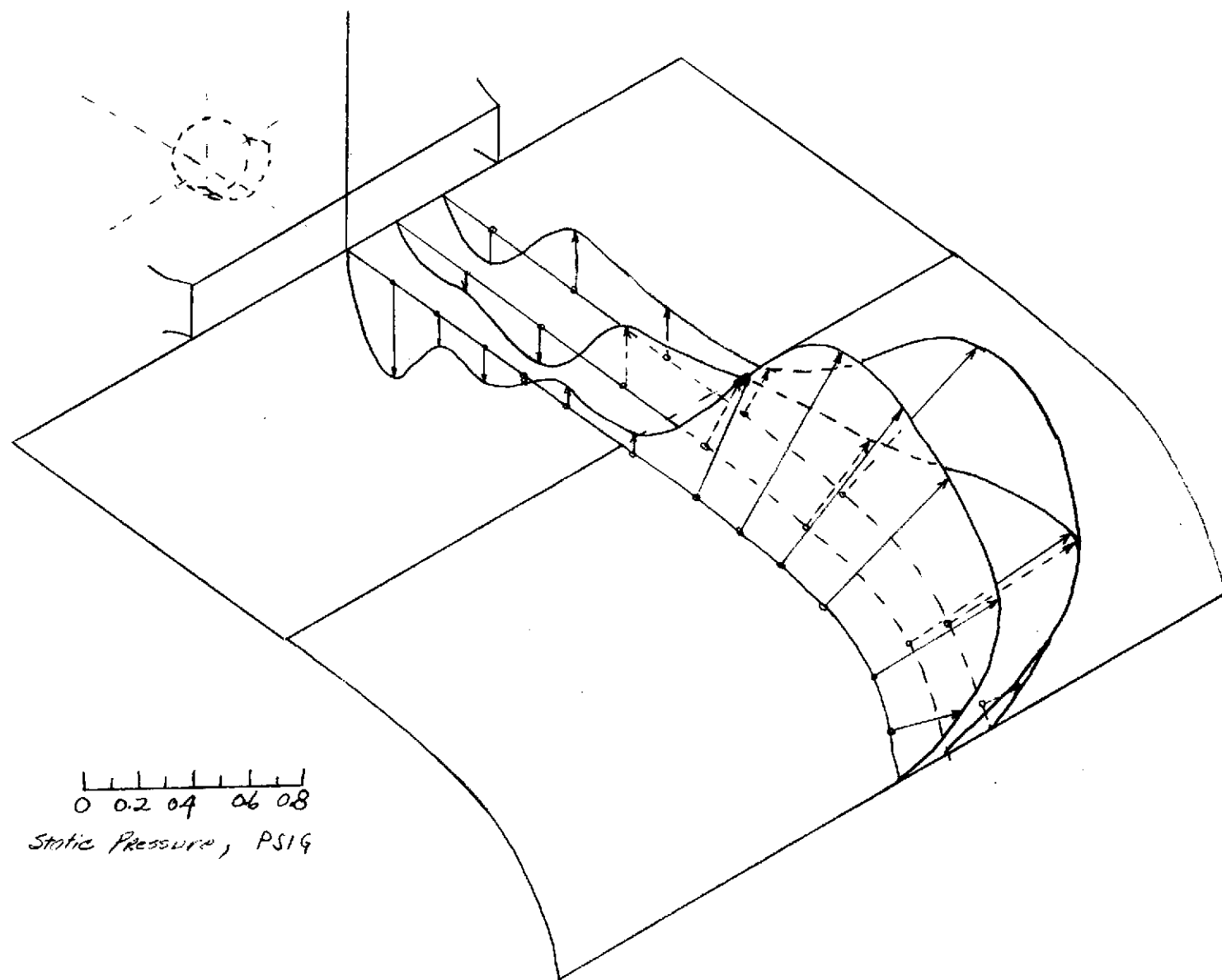


0 0.2 0.4 0.6 0.8

Static pressure, PSIG

(b) $\alpha_f = 29.8^\circ$

FIGURE 11 -- CONT'D



0 0.2 0.4 0.6 0.8
Static Pressure, PSIG

33

FIGURE 11 - CONT'D.

(C) $\delta_f = 50.8^\circ$

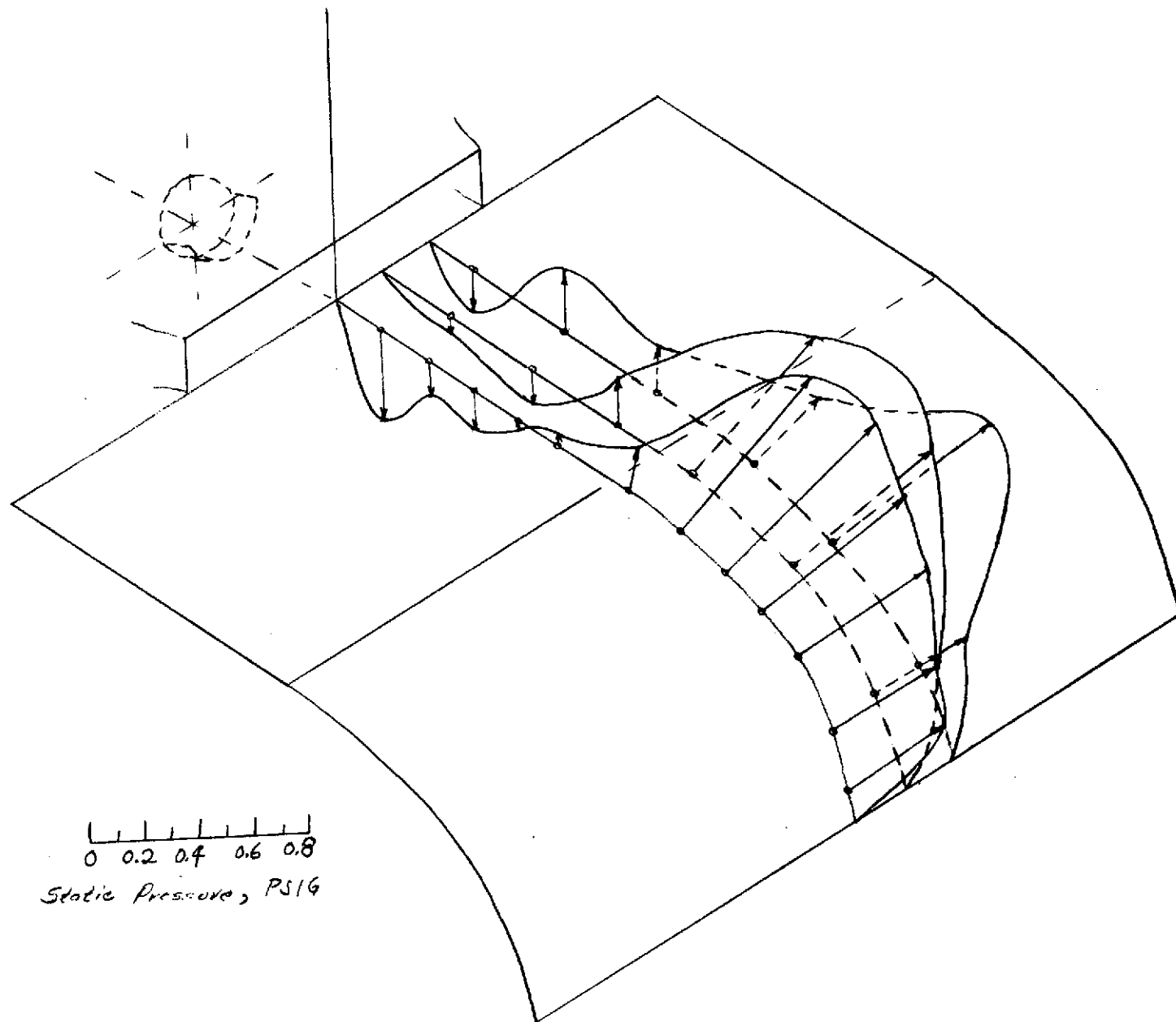
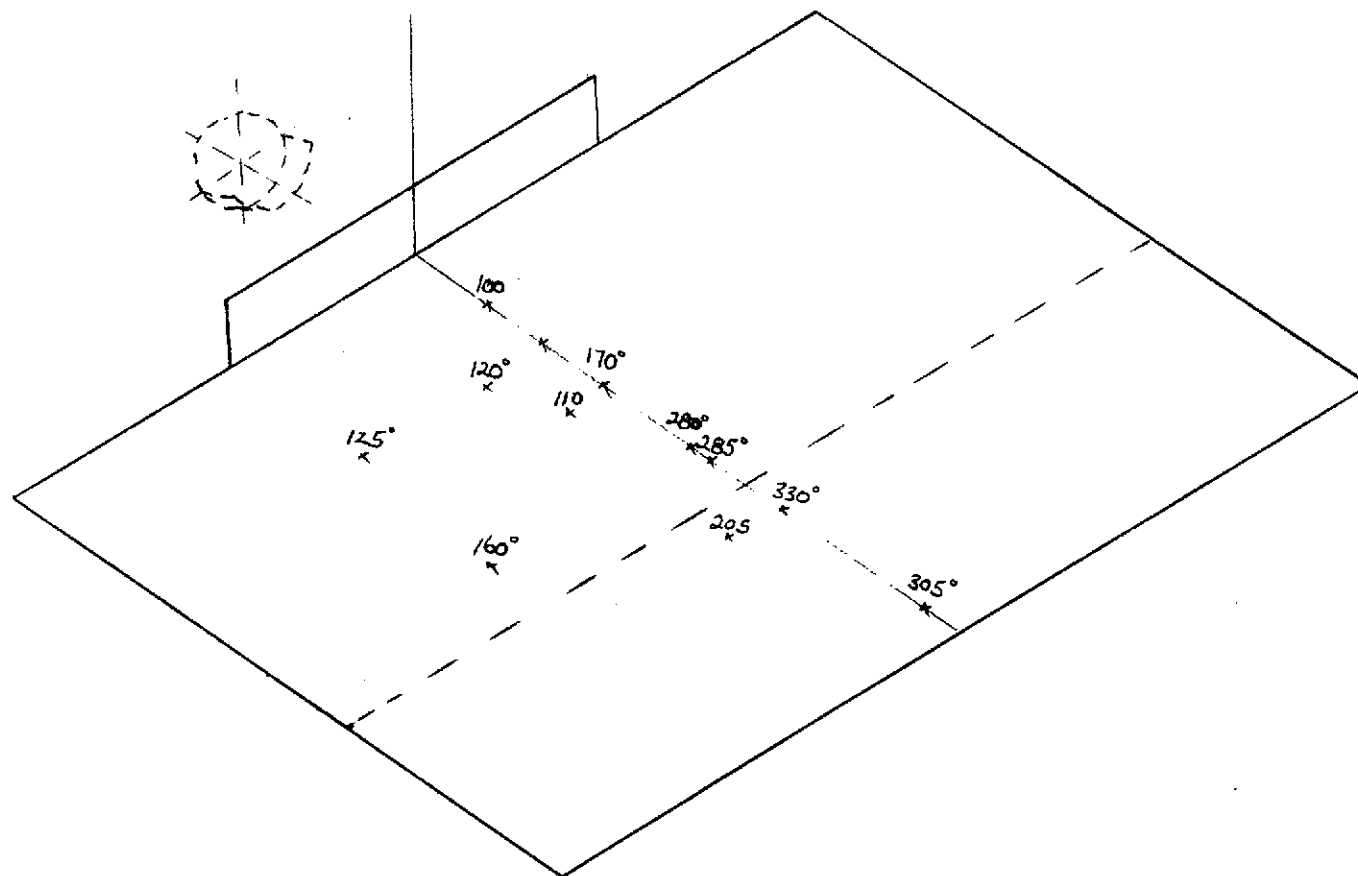


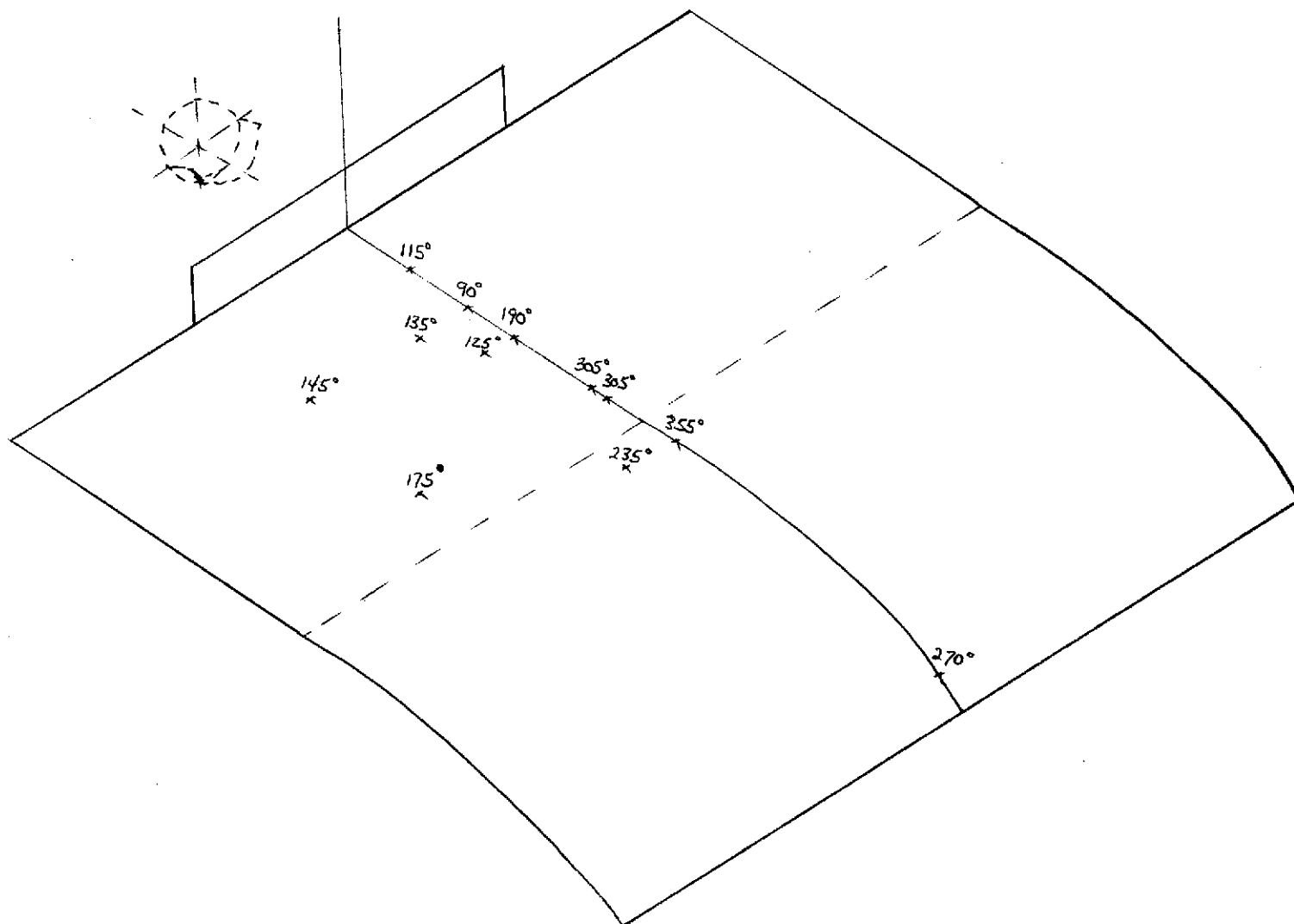
FIGURE 11 - CONCLUDED.

(d) $\delta_f = 70^\circ$



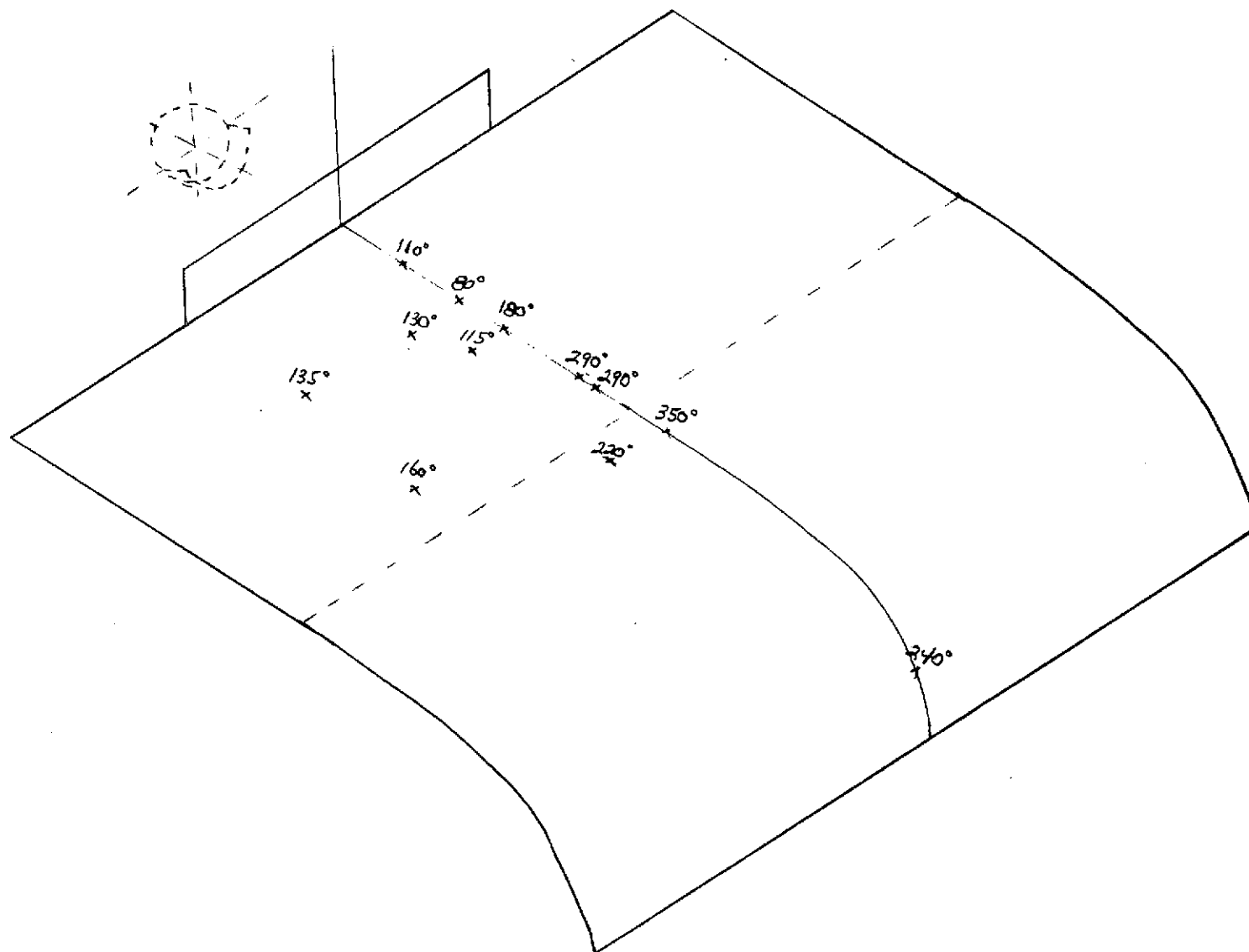
(a) $\delta_f = 9.2^\circ$

FIGURE 13 -- SURFACE TEMPERATURE OVER WING AND FLAP, deg F. Round Primary #033¹⁰ with deflector. 1920 lbs. THRUST.



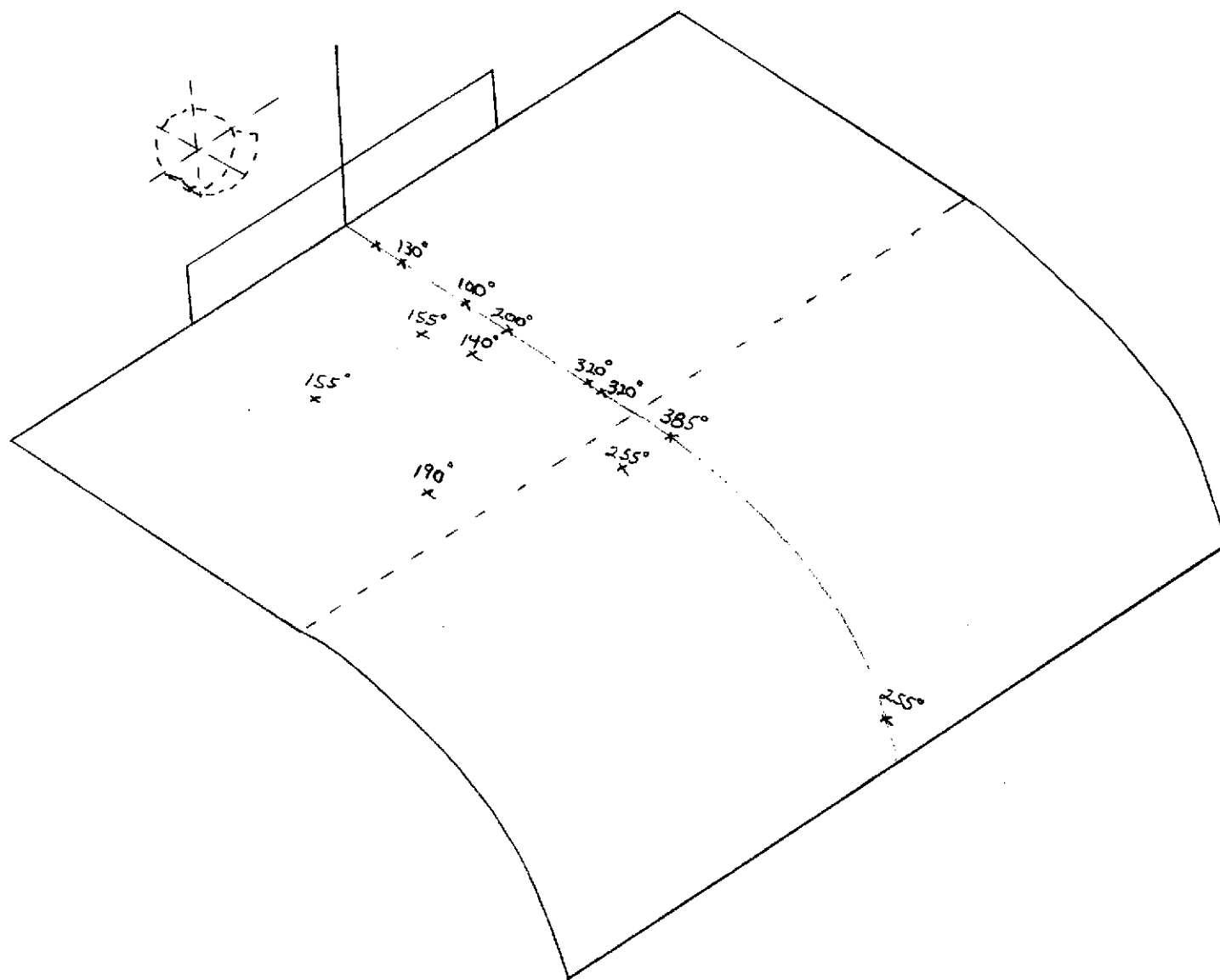
(b) $\angle_f = 29.8^\circ$

FIGURE 13 - CONT'D



(C) $\angle_f = 50.8^\circ$

FIGURE 13 -- CONT'D



(d) $d_f = 70^\circ$

FIGURE 13 - CONCLUDED.

27

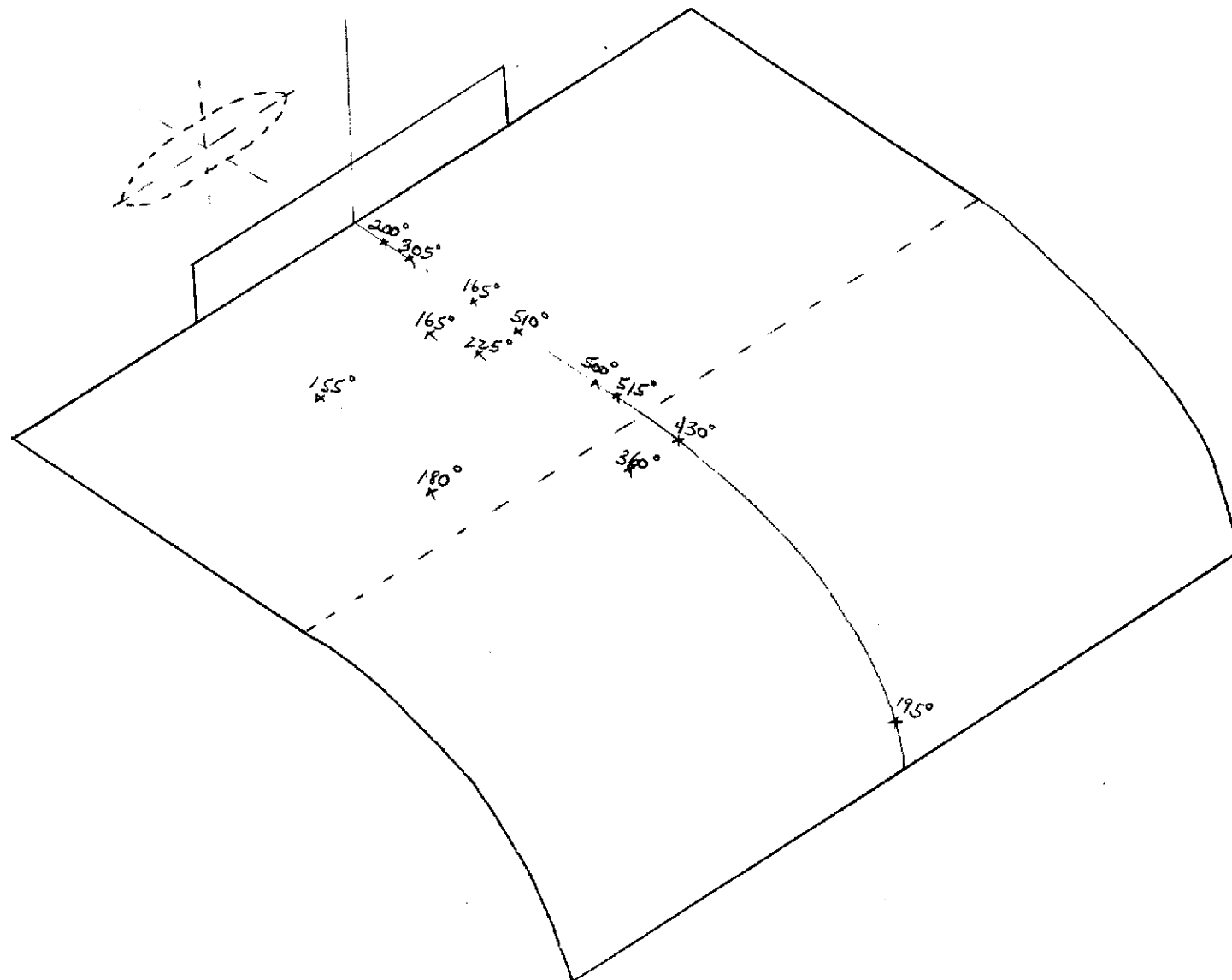


FIGURE 14 - SURFACE TEMPERATURE OVER WING AND FLAP, $\alpha_p F = 111$ ft/min primary no 331c; 1920 lbs. THRUST. $\beta_f = 70^\circ$.

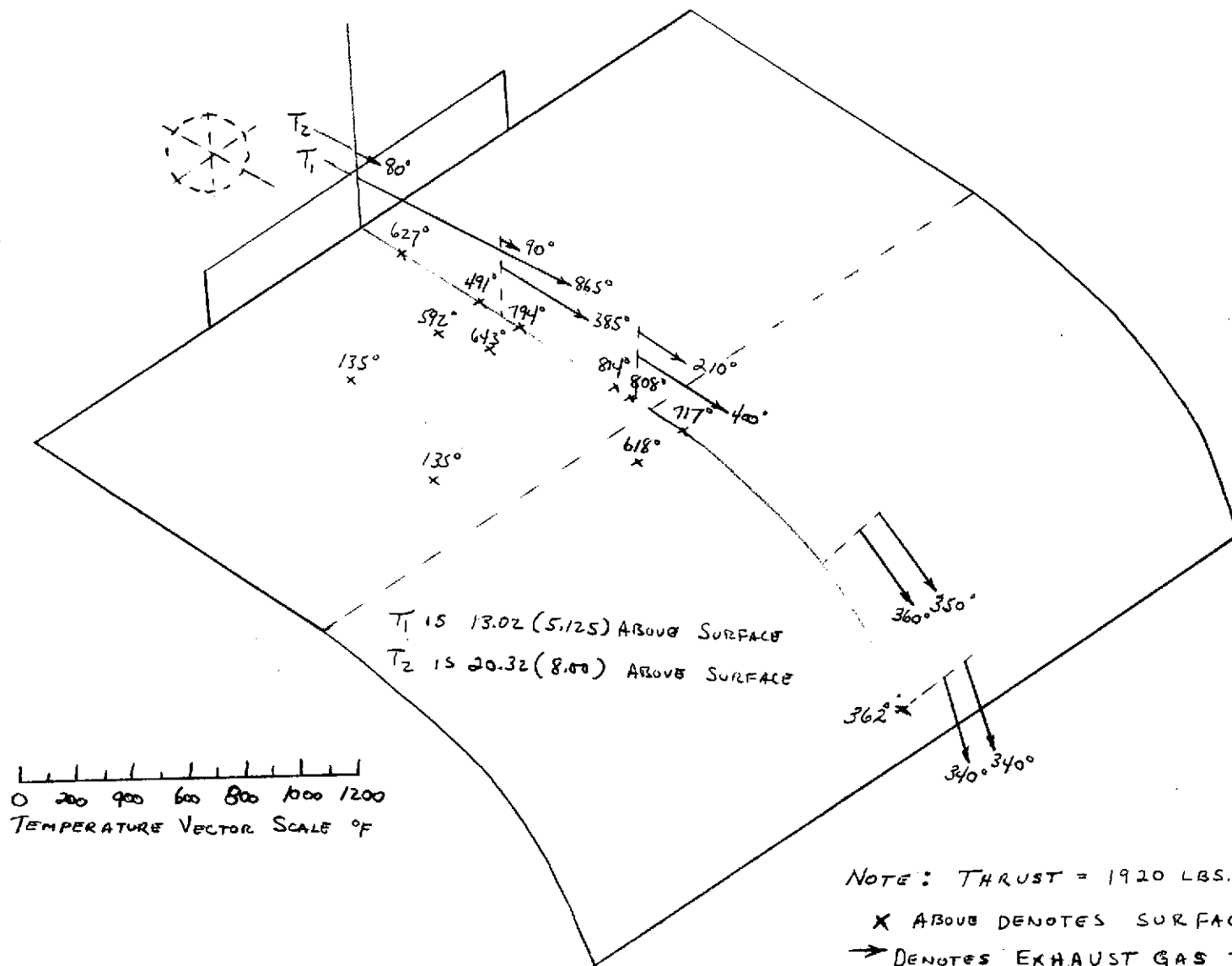


FIGURE 15 -- TEMPERATURE OF EXHAUST GAS EFFLUX ON EXHAUST EXIT CENTERLINE AT 5 CHORDWISE STATIONS. SURFACE TEMPERATURE AVERAGED FOR 5 RUNS. BASIC ROUND PRIMARY NOZZLE; $\phi = 70^\circ$. DIMENSIONS ARE IN CENTIMETERS (INCHES)

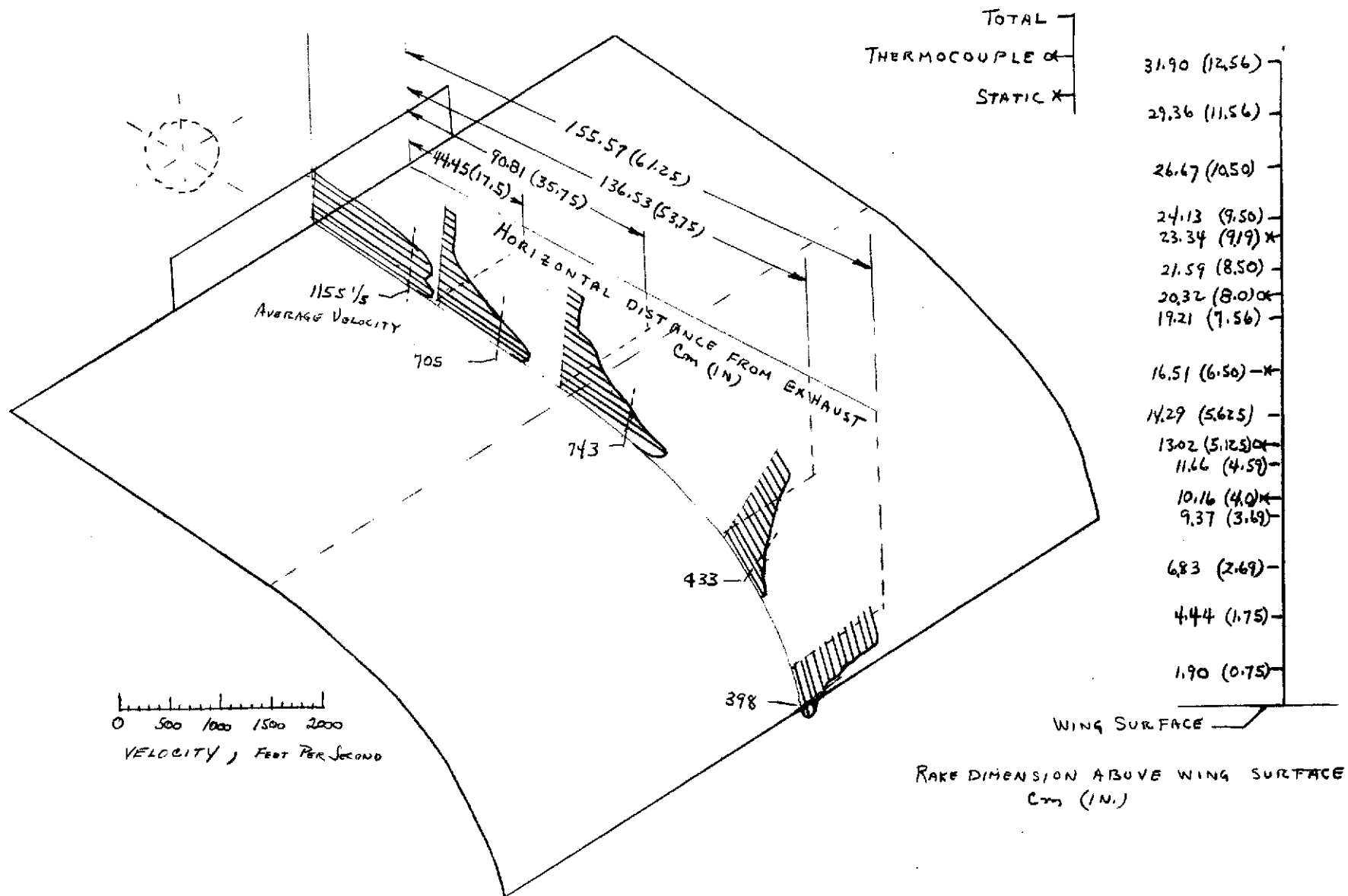


FIGURE 16-- VELOCITY PROFILE ABOVE THE WING AND FLAP AT FIVE CHORDWISE STATIONS; BASIC ROUND PRIMARY NOZZLES; $\delta_f = 70^\circ$; THRUST = 1920 lbs.